Mixture effects of pharmaceuticals carbamazepine, diclofenac and venlafaxine on *Mytilus galloprovincialis* mussel probed by metabolomics and proteogenomics combined approach

Thibaut Dumas, Elena Gomez, Julien Boccard, Gaëlle Ramirez, Jean Armengaud, Aurélie Escande, Olivier Mathieu, Hélène Fenet, Frédérique Courant

Mixture effects of pharmaceuticals carbamazepine, diclofenac and venlafaxine on *Mytilus galloprovincialis* mussel probed by metabolomics and proteogenomics combined approach

Thibaut Dumas [a], Elena Gomez [a], Julien Boccard [b,c], Gaëlle Ramirez [a], Jean Armengaud [d], Aurélie Escande [a], Olivier Mathieu [a,e], Hélène Fenet [a] and Frédérique Courant [a*]

[a] HydroSciences Montpellier, IRD, CNRS, University of Montpellier, Montpellier, France;
[b] School of Pharmaceutical Sciences, University of Geneva, Geneva 1211, Switzerland;
[c] Institute of Pharmaceutical Sciences of Western Switzerland, University of Geneva, Geneva 1211, Switzerland
[d] Université Paris-Saclay, CEA, INRAE, Département Médicaments et Technologies pour la Santé (DMTS), SPI, Bagnols-sur-Cèze, France;
[e] Laboratoire de Pharmacologie-Toxicologie, CHU de Montpellier, Montpellier, France

* Corresponding author at: HydroSciences Montpellier, IRD, CNRS, University of Montpellier, 15 avenue Charles Flahault, 34093 Montpellier, France. E-mail address: frederique.courant@umontpellier.fr

Abstract

Exposure to single molecules under laboratory conditions has led to a better understanding of the mechanisms of action (MeOAs) and effects of pharmaceutical active compounds (PhACs) on non-target organisms. However, not taking the co-occurrence of contaminants in the environment and their possible interactions into account may lead to underestimation of their impacts. In this study, we combined untargeted metabolomics and proteogenomics approaches to assess the mixture effects of diclofenac, carbamazepine and venlafaxine on marine mussels (*Mytilus galloprovincialis*). Our multi-omics approach and data fusion strategy highlighted how such xenobiotic cocktails induce important cellular changes that can be harmful to marine bivalves. This response is mainly characterised by energy metabolism disruption, fatty acid degradation, protein synthesis and degradation, and the induction of endoplasmic reticulum stress and oxidative stress. The known MeOAs and molecular signatures of PhACs were taken into consideration to gain insight into the mixture effects, thereby revealing a potential additive effect. Multi-omics approaches on mussels as sentinels offer a comprehensive overview of molecular and cellular responses triggered by exposure to contaminant mixtures, even at environmental concentrations.

Keywords: multi-omics; proteomics; pharmaceutical active compounds; bivalve mollusks; data fusion; adverse effects

1. Introduction

Pharmaceutical active compounds (PhACs) include a vast diversity of molecules, thousands of which are marketed worldwide. However, it is now recognized that large consumption and release of these compounds can potentially pose a threat to aquatic environments, including marine ecosystems (Fabbri and Franzellitti, 2016; Mezzelani et al., 2018; Santos et al., 2010). Commonly prescribed PhACs are consequently often detected in the marine environment including the antiepileptic carbamazepine (CBZ), the nonsteroidal anti-inflammatory drug (NSAID) diclofenac (DCF) and the antidepressant venlafaxine (VLF) (Arpin-Pont et al., 2016; Branchet et al., 2021; Desbiolles et al., 2018; Fernández-Rubio et al., 2019; Moreno-González et al., 2016; Sousa et al., 2020). For instance, Sousa et al. (2020) detected DCF in 20 out of 36 estuarine water samples, which is the highest frequency among the other targeted PhACs. Other authors showed in their study a highest detection frequency for VLF found in 59% of coastal water samples (Fernández-Rubio et al., 2019). In addition, CBZ is known for its low removal in wastewater treatment plants (Margot et al., 2015) and its low (bio)degradability in the environment (Benotti and Brownawell, 2009; Calisto et al., 2011). For these reasons, CBZ has been proposed as a possible anthropogenic marker of urban pollution in the aquatic systems (Clara et al., 2004; Hai et al., 2018). Their concentration in marine ecosystems ranges from <1 to 1410 ng/L for CBZ (Almeida et al., 2021), from <1 to hundreds ng/L for DCF (Bonnefille et al., 2018b) and, from <1 to few hundreds ng/L for VLF (see references in Ramirez et al., 2022). These PhACs have also been measured in the tissues of filter feeders, such as bivalves, at few ng/g dry weight, up to >10 ng/g (Almeida et al., 2021; Alvarez-Muñoz et al., 2015; Bonnefille et al., 2018b; Martínez Bueno et al., 2013, 2014). In addition, metabolites of these PhACs have been quantified after the exposure of bivalves to the parent compounds in laboratory studies (Ariza-Castro et al., 2021; Boillot et al., 2015; Bonnefille et al., 2017;

57 Gomez et al., 2021), thus indicating the ability of these organisms to metabolize them. This situation
58 raises the question of the effects that PhACs may have on these non-target organisms.
59 Research has shown that PhACs can affect non-target organisms via the mechanism(s) of action
60 (MeOA) for which they were designed, as many biological targets are conserved across organisms. For
61 instance, some carbamazepine (CBZ) MeOAs known in humans have also been reported in marine
62 bivalves: CBZ leads to a reduction in intracellular cAMP levels by interacting with the adenylyl cyclase
63 system (Martin-Diaz et al., 2009), has a potential gamma-aminobutyric acid (GABA) receptor agonist
64 role (Almeida et al., 2018), interacts with voltage-dependent Na^+ and K^+ channels (Freitas et al., 2016)
65 and, may also induce autophagy through either endoplasmic reticulum (ER) stress induction or inositol
66 monophosphatase inhibition (Dumas et al., 2022a). For diclofenac (DCF), its main MeOA in humans is
67 cyclooxygenase COX-1 and COX-2 inhibition, which decreases prostaglandin E2 (PGE2) and
68 thromboxane production. This MeOA seems to be conserved in marine mussels (*Mytilus*
69 *galloprovincialis*), as suggested by a diminution in PGE2 after DCF exposure (Courant et al., 2017).
70 Similarly, an increase of serotonin was measured in marine mussels following exposure to VLF, an
71 antidepressant classified as a serotonin-norepinephrine reuptake inhibitor (SNRI) in humans (Ramirez
72 et al., 2022). These studies confirmed that PhACs act on non-target organisms through conserved
73 MeOAs, although unexpected MeOAs could also be involved due to biological differences between
74 species. Marine organism exposure to such PhACs could thus elicit adverse physiological effects. For
75 instance, DCF, CBZ and VLF are known to individually trigger oxidative stress, immunotoxicity and
76 genotoxicity in marine molluscs, thereby causing a decrease in their feeding activity and impairing
77 byssus production in mussels (Almeida et al., 2020; Bonnefille et al., 2018b; Fong et al., 2015; Lacaze
78 et al., 2015). Our previous studies on each individual compound also demonstrated metabolic and
79 cellular responses triggered by exposure in *M. galloprovincialis*. DCF disturbed the metabolism of
80 tyrosine (e.g. catecholamines) and tryptophan (e.g. serotoninergic related compounds), with a risk for
81 impaired reproduction and osmoregulation of mussels (Bonnefille et al., 2018a). Exposure to CBZ
82 involved a disruption of lipid and amino acid metabolisms and, an intensification of protein synthesis

as well as of transport and catabolism processes (Dumas et al., 2022a). These molecular signatures indicate a cytotoxic effect of CBZ induced by several mechanisms. VLF triggered the modulation of hundreds metabolites belonging to the metabolism of amino acids (e.g. phenylalanine, tyrosine, tryptophan, arginine, etc.), purine and pyrimidine metabolisms (adenosine, cyclic AMP, thymidine, etc.), as well as serotonin directly related to its MeOA, and many other metabolites involved in diverse functions (Ramirez et al., 2022). Such molecular disturbances induced by VLF could have an impact on the reproduction and behavior of mussels. All three PhACs thus affect marine organisms through toxicological pathways that are still only partially understood on the basis of the findings of studies conducted under individual laboratory exposure conditions.

CBZ, DCF and VLF co-occur in marine ecosystems and are also jointly detected in marine organism tissues (Desbiolles et al., 2018; Moreno-González et al., 2016), but the effects of mixture of these PhACs have yet to be investigated. Mixture effects in the environment (e.g. treated wastewater) can be additive when PhACs act independently or through the same MeOA, or synergistic or antagonistic when they interfere with each other (Backhaus, 2014; Dumas et al., 2020b; Eggen et al., 2004). Examples of such mixture effects are highlighted in the review of Godoy and Kummrow (2017) concerning almost 200 assessments of mixture toxicity from 65 reported studies. However, most assessments of mixture effects on organisms relied solely on target-oriented effect approaches without considering the mechanism of action (i.e. ecotoxicological tests such as growth, luminescence or reproduction inhibition, survival/mortality, etc.). For instance, Di Nica et al. (2017) showed the clear presence of synergistic effects of several binary PhAC mixtures, such as diclofenac-chlortetracycline, by measuring the bioluminescence inhibition response of *Aliivibrio fischeri* marine bacteria. Although those approaches are suitable for predicting and assessing the effects of PhAC mixtures through concentration addition or independent action models, they provide little mechanistic information on toxicity pathways and may overlook unexpected joint effects. Moreover, studies considering PhAC mixture effects on marine organisms, such as filter feeders (e.g. bivalves), are still sparse (Almeida et al., 2022; Cunha et al., 2023).

Omics approaches could help shed light on a broad range of molecular changes triggered by such exposures, especially at the transcriptome, proteome and metabolome levels (Martins et al., 2019). Building on its potential, harnessing omics holds the key to unlocking deeper insights into the intricate molecular mechanics of PhAC mixtures (Kidd et al., 2023). In the last two decades, environmental metabolomics has proven effective in ecotoxicology research (Castaño-Ortiz et al., 2023; Chan et al., 2023; De Marco et al., 2023; Labine et al., 2023), with advances achieved in assessing contaminant MeOAs, especially when combined with other omics approaches such as proteomics (recently reviewed in Dumas et al., 2022b). Multi-omics offer a key tool for in-depth exploration of molecular processes involved in responses to contaminant exposure. Furthermore, to be able to take full advantage of multi-omics approaches, it is essential to implement an adapted data fusion strategy in order to highlight correlated signatures between different omics levels (e.g. metabolites and proteins). Such a strategy enables the integrative analysis of different omics dataset despite a certain degree of heterogeneity between large-scaled approaches and the intrinsic complexity of the generated datasets. In our previous study, we successfully applied a mid-level data fusion strategy combining metabolomics and proteogenomics data (detailed in Dumas et al., 2022a). The complementarity between these two omics levels enhances confidence in the metabolic pathways and cellular processes affected by contaminants, which is a major beneficial feature of this strategy. For instance, proteomics provides access to functional information on proteins, which may allow us to put forward hypotheses on the affected molecular and cellular processes, while the detection of modulated metabolite end products of biochemical reactions could support these hypotheses if they are directly or indirectly related to these processes. To explore mixture effects at the MeOAs level, it is worthwhile to harness the complementarity of omics through their combination. To date, only a few multi-omics approaches have been applied to study mixture effects on aquatic organisms (Dondero et al., 2010; Song et al., 2016; Vandenbrouck et al., 2009).

The present study was designed to investigate the mixture effects of CBZ, DCF and VLF in Mediterranean mussels (*M. galloprovincialis*) through an integrated metabolomics and

proteogenomics approach based on a mid-level data fusion strategy. We focused on a mixture of PhACs with different therapeutic classes, i.e. not sharing known MeOAs. We assumed that no interactions would occur at the molecular targets related to their MeOAs and hence expected to observe each individual PhAC signature, as noted in our previous studies (DCF: Bonnefille et al., 2018a; CBZ: Dumas et al., 2022a; VLF: Ramirez et al., 2022) and also reported in the literature.

2. Materials & Methods

2.1. Chemicals

LC-MS-grade solvents (acetonitrile, formic acid, dichloromethane, and methanol) were obtained from CARLO ERBA Reagents (Val de Reuil, France). Ultrapure water was generated by a Simplicity® Water Purification System associated with an LC-Pak® Polisher and a Millipak® Express 20 filter (0.22 µm) from Merck Millipore (Bedford, MA, USA). Pure analytical grade standards (purity > 95%) were purchased from the following suppliers: Sigma-Aldrich (now part of MERCK, Saint-Quentin-Fallavier, France), Santa Cruz Biotechnology (Santa Cruz, CA, USA), and Toronto Research Chemicals (Toronto, ON, Canada).

2.2. Animals, experimental design and sample collection

Mytilus galloprovincialis mussels were provided by Les Compagnons de Maguelone mussel farmers (Villeneuve-les-Maguelone, France) in February 2020. Mussels were transported in a mesh bag to the laboratory within an hour at ambient outside temperature (14°C). Mussels (n = 105 individuals) with a homogeneous shell size (7 cm ± 0.8) were cleaned and randomly distributed in 14 glass aquaria (5 individuals per aquarium). Each aquarium contained 2 L of filtered seawater (filter GF/F Ø 100 µm) provided by IFREMER (Palavas, France). Seawater was continuously aerated and renewed daily (static renewal). Mussels were fed once daily with the *Tetraselmis suecica* algae (Greensea, Mèze, France) at constant density (21,000 cells/mL) and we ensured that algae uptake was complete within 1 h. Throughout the experiment, seawater physicochemical parameters were checked daily and

maintained constant: temperature (13.8 °C ± 0.5), oxygen (10 mg/L ± 0.3), salinity (36.7‰ ± 0.2) and pH (8.07 ± 0.05).

After a 7-day acclimatization period, 6 aquaria underwent solvent control exposure (10 µL/L of methanol, corresponding to a final dilution of 0.01‰; SC), 6 aquaria were exposed to the mixture (CBZ, DCF and VLF) at a low nominal concentration of 0.1 µg/L (LD), and 6 aquaria were exposed to the mixture at a higher nominal concentration of 10 µg/L (HD). The low concentration has been chosen in order to get closer to environmental conditions and the higher concentration to 'magnify' certain effects which would have escaped us at low concentration and which would give us a better understanding of MeOAs and potential interactions. To quantify the PhACs exposure, the water was sampled every days throughout the experiment, just after the aquaria had been spiked. The methods of quantification have been published in our previous works (Bonnefille et al., 2018a; Dumas et al., 2022a; Ramirez et al., 2022). The concentrations measured were as follows: DCF = 0.139 ± 0.057 µg/L and 10.69 ± 1.71 µg/L; VLF = 0.087 ± 0.034 µg/L and 7.48 ± 2.25 µg/L; CBZ = 0.079 ± 0.018 µg/L and 10.05 ± 0.87 µg/L. During the exposure period, mixture concentrations were re-established daily 1 h after seawater renewal and mussel feeding to prevent any compounds adsorption on algae. No mortality was recorded during the 7-day exposure period. Genetic determination of the species confirmed the absence of hybridization between *Mytilus galloprovincialis* and *Mytilus edulis* (Laboratory TOXEM, Montivilliers, France).

Commenté [FC1]: Tous les jours ? Tous les deux jours ?

Commenté [DT2R1]: Il me faut vérifier

Commenté [DT3R1]: J'ai rajouté tous les jours

Mussels were collected for dissection at the end of the exposure period. The digestive glands and the remaining soft tissues were frozen at -80°C in cryotubes prior to analysis. In order to avoid any bias due to the sex confounding factors, as males and females can respond differently to contaminant exposures (Dumas et al., 2020a; Ramirez et al., 2022), the sex of mussels was determined. Microscopic analysis of a gonadal smear allowed us to identify the presence of spermatozoa or oocytes and thus define the sex of the individuals. We identified 17 males and 18 females in SC exposure conditions; 16 males and 19 females in LD exposure conditions, and 22 males and 13 females in HD exposure

conditions. Only male mussel samples were used for subsequent analyses because of the greater number of males identified per condition with sufficient material to carry out both metabolomic and proteogenomics analyses on the same sample. Twelve samples from each exposure condition were prepared for omics analyses, thereby ensuring suitable statistical conditions.

2.3. Metabolomics analysis

2.3.1. Sample preparation

Frozen digestive glands of male mussels were freeze-dried using the Heto powerDry LL3000 (Thermo Fisher Scientific), and then ground into powder. As described in previous studies (Bonnefille et al., 2018a; Dumas et al., 2022a; Ramirez et al., 2022), 30 mg of powder was homogenized in 240 µL of methanol and 75 µL of ultrapure water was added and further vortexed for 60 sec. Then 240 µL of dichloromethane and 120 µL of ultrapure water were added and vortexed for 60 sec. The samples were left on ice for 15 min, vortexed, and centrifuged at 2,000×g for 15 min at 4°C. Then, 50 µL of the supernatant was transferred into glass tubes and evaporated to dryness under a nitrogen stream at 35°C with a TurboVap® LV concentration workstation from Caliper LifeSciences (Waltham, MA, USA). The extracts were re-suspended in 200 µL of water/acetonitrile (95/5; *v*/*v*), and then filtered into centrifugal devices with a 10 kDa cut-off (VWR, Fontenay-sous-Bois, France). The filtrates were finally transferred into vials prior to liquid chromatography–high resolution mass spectrometry (LC-HRMS) analysis.

2.3.2. Data acquisition and quality control

LC-HRMS untargeted analysis was performed on a Thermo Scientific Vanquish™ Quaternary HPLC system (Waltham, MA, USA) coupled with a Thermo Scientific Q Exactive™ Focus Hybrid Quadrupole-Orbitrap mass spectrometer equipped with a heated electrospray ionization (HESI) probe.

HPLC separation was performed with a reverse phase pentafluorophenylpropyl (PFPP) analytical column (100 × 2.1 mm; 3 µm particle size; Sigma Aldrich, PA, Bellefonte, USA). Each sample (10 µL) was loaded onto the column with full loop injection. Mobile phases were mixtures of

water/acetonitrile (99:1, *v*/*v*) (phase A) or water/acetonitrile (1:99, *v*/*v*) (phase B) spiked with 0.1% of formic acid. The flow rate was set at 250 µL/min, and a gradient elution was started with 5% B until 3 min, increased until 40% B at 8 min, 50% B at 9 min, 70% B at 13 min, to reach 95% B at 15 min until 18 min, and then returned to starting conditions 5% B at 21 min, followed by a 7-min re-equilibration period.

The Q-Exactive™ Focus HRMS was adjusted to a mass resolution of 35,000 (FWHM, m/*z* 200) with a mass range of 50–750 *m*/*z*. Samples were analyzed simultaneously in positive and negative electrospray ionization modes (ESI+ and ESI-, respectively) using polarity switching mode with the following settings: spray voltage 3.35 |kV|, sheath gas flow rate 55, gas flow rate 10, S-Lens RF level 50, capillary temperature 300°C and heater temperature 250°C. The sample injection order was randomly determined to reduce the influence of potential confounding factors. MS/MS acquisitions were performed on QC samples with a high energy collision dissociation cell set at 20 eV with a mass resolution of 17,500.

A quality control (QC) sample corresponding to a pool of 30 µL of each sample extract was injected 10 times at the beginning of the analytical sequence to equilibrate the column. QC injections were repeated throughout the sequence to monitor the analytical repeatability and sensitivity. Relative standard deviations (RSD) were calculated for each ion detected in the QC samples to assess the injection repeatability. An analytical variability control was set such that 70% of ions had to have an RSD <30% (Want et al., 2010).

2.3.3. Data pre-processing

The raw data files were converted into mzXML files with MSConvert freeware (ProteoWizard 3.0) (Kessner et al., 2008). A multi-step strategy was applied for processing ESI+ and ESI- acquisitions separately using the XCMS package (Smith et al., 2006) in the R environment. Optimized XCMS parameters were implemented as follows: the *m*/*z* interval for peak picking was set at 0.0025, the signal-to-noise ratio threshold was set at 10, the group bandwidth was set at 8, and the minimum

234 fraction was set at 0.5. XCMS returned results as a peak table with variable identity (i.e. *m/z* and
235 retention time) and feature abundances (i.e. peak area). After visual inspection of each extracted ion
236 chromatogram, all features corresponding to baseline drift or background noise were discarded from
237 the peak table. In addition, the CAMERA Bioconductor package (Kuhl et al., 2012) was used to remove
238 isotopes, adducts, and fragments from the peak table, thus avoiding information redundancy. Based
239 on QC sample injections, only features with an RSD < 30% were kept for further data processing and
240 annotation.

241 *2.3.4. Metabolite annotation and identification*

242 Metabolite annotation was carried out by mass-matching with 0.002 Da precision using the
243 Human Metabolome Database (HMDB; http://www.hmdb.ca/; (Wishart et al., 2013)). The annotation
244 confidence levels were defined according to the recommendations of the Compound Identification
245 work group of the Metabolomics Society (Blaženović et al., 2018): (i) level 1 corresponded to
246 unambiguous identifications based on the accurate mass and retention time of the corresponding
247 analytical standard injected under the same analytical conditions (in-house database based on more
248 than 300 metabolites belonging to amino acids, nucleotides, carbohydrates, lipids, cofactors and
249 vitamins), and (ii) level 2 corresponded to putative annotations based upon physicochemical
250 properties and/or spectral similarity of MS/MS spectra with public databases (HMDB and mzCloud).

251 *2.3.5. Differential metabolite abundance analysis*

252 Differential metabolite abundance between the solvent control conditions and the CBZ-DCF-
253 VLF mixture treated conditions (SC *vs* LD or SC *vs* HD) was assessed with a Welch t-test. The false
254 discovery rate (FDR) was controlled using the Benjamini–Hochberg FDR correction. Metabolites with
255 an absolute significant modulation > 30% and an adjusted p-value < 0.05 were considered statistically
256 relevant. Modulation trend can also be of interest (p-value < 0.1). The rational to set this threshold
257 was driven by the potential to uncover a biological modulation trend resulting from the exposure.
258 Focusing on individual metabolites in isolation represents a somewhat simplified perspective of

metabolic changes that encompass intricate interconnections within metabolic pathways. In fact, observing a trend ($p < 0.1$) indicating either a decrease or increase in multiple metabolites within the same pathway, thereby highlighting a disturbance in the biochemical cascade, might hold more biological significance than relying solely on a single marker metabolite ($p < 0.05$).

2.3.6. Metabolic pathway analysis

Pathway analysis was performed on MetaboAnalyst 5.0 (Xia and Wishart, 2010) in order to highlight significantly impacted metabolic pathways. The Pathway analysis tool integrates both a pathway enrichment analysis and a pathway topology analysis. The settings used are as follows: hypergeometric test for enrichment method and relative-betweenness centrality for topology analysis.

2.4. Proteogenomics analysis

2.4.1. Protein extraction

Powder of each lyophilized digestive gland (7 mg) was mechanically homogenized by bead-beating in 70 µL of LDS sample buffer (Invitrogen, Fisher Scientific, Illkirch, France) with a Precellys Evolution sample homogenizer (Bertin Technologies, Montigny-le-Bretonneux, France). The homogenates were centrifuged at 10,000×g for 3 min in order to pellet the cellular debris, and the resulting supernatant was transferred to a new tube. As previously recommended (Hayoun et al., 2019), samples were homogenized with a mix of 0.1 mm and 0.5 mm glass beads and 0.1 mm silica beads. Five homogenization cycles at 6,800 rpm with a 30 s pause between each were necessary to achieve complete dissolution of the material. Centrifugation at 16,000×g for 2 min was performed, and samples were then incubated at 99°C for 5 min and briefly centrifuged. A 20 µL aliquot of each supernatant was then subjected to SDS-PAGE for a short electrophoretic migration, as described previously (Trapp et al., 2015). The whole-protein content from each well was extracted as a single polyacrylamide band, processed as described (Hartmann et al., 2014), and submitted to proteolysis with trypsin (Roche) using 0.01% ProteaseMAX surfactant (Promega).

283 *2.4.2. Liquid chromatography - tandem mass spectrometry method*

284 Shotgun proteomics peptide analysis was carried out using a Q Exactive HF mass spectrometer
285 (ThermoFisher Scientific) coupled with an UltiMate 3000 LC system (Dionex-LC Packings). The
286 analytical method was previously described in Klein et al. (2016). Briefly, peptides were resolved onto
287 a nanoscale C18 PepMapTM 100 capillary column (LC Packings) at a 0.2 µl/min flow rate with a 90-min
288 gradient of acetonitrile and 0.1% formic acid. A Top20 data-dependent method was used, which
289 consisted of scan cycles involving a full scan of peptide ions in the Orbitrap analyzer, followed by high-
290 energy collisional dissociation and MS/MS scans on the 20 most abundant precursor ions. Full scan
291 mass spectra were acquired from *m*/*z* 350 to 1,800 at 60,000 resolution. Ion selection for MS/MS
292 fragmentation and measurement was performed by applying a 10 s dynamic exclusion window.

293 *2.4.3. Peptide assignation and proteomics data analysis*

294 MS/MS spectra were assigned to peptide sequences by the MASCOT Daemon 2.3.2 search
295 engine (Matrix Science, London, UK), with searches performed against the digestive gland specific
296 RNAseq-derived database obtained by *de novo* assembly with Trinity version 2.4 (Haas et al., 2013),
297 followed by ORF search and transcript translation with Transdecoder, as described in Cogne et al.
298 (2019). The final protein database contained 86,022 putative protein sequences totaling 29,583,007
299 amino acids, as reported in Dumas et al. (2022). For MS/MS spectra assignment, the parameters were:
300 full-trypsin specificity, maximum of one missed cleavage, mass tolerance of 5 ppm on the parent ion
301 and 0.02 Da on the MS/MS, carboxyamidomethylated cysteine (+57.0215) as a fixed modification, and
302 oxidized methionine (+15.9949) and deamidation of asparagine and glutamine (+0.9848) as variable
303 modifications. All peptide matches presenting a MASCOT ion score with a p-value of < 0.05,
304 corresponding to an FDR of 1% as evaluated with the DecoyPyrat procedure (Wright and Choudhary,
305 2016), were filtered and assigned to a protein based on a parsimony rule (with at least two different
306 peptides, one of which was unique). Functional annotation of identified proteins was performed by
307 sequence similarity search using Swissprot and NCBInr databases with the DIAMOND tool alignment,

as previously described (Trapp et al., 2018). Peptide-to-spectrum matches were counted for each protein leader of the protein group defined on the basis of their sequence similarities.

2.4.4. Mass spectrometry and proteomics data

The mass spectrometry proteomics data were deposited to the ProteomeXchange Consortium via the PRIDE (Perez-Riverol et al., 2019) partner repository with the dataset identifier PXD045957 and project 10.6019/PXD045957.

2.4.5. Differential protein abundance analysis

For each validated protein, the number of spectral counts was used as a proxy of their relative abundances and was normalized, as described in Liu et al. (2004). Differential protein abundance between the solvent control condition and the CBZ-DCF-VLF mixture treated conditions (SC *vs* LD or SC *vs* HD) was assessed with a Student *t*-test, followed by a Benjamini-Hochberg correction of the p-value. Proteins with an absolute significant modulation > 40% and an adjusted p-value < 0.05 were considered as differentially expressed between the solvent control condition and the treated conditions.

2.4.6. Function and pathway enrichment analysis

Gene Ontology (GO) term enrichment analysis was performed on the STRING database (Szklarczyk et al., 2019; https://string-db.org/). Enrichment analysis of Kyoto Encyclopedia of Genes and Genomes (KEGG) pathways was performed using a web-based tool, i.e. the KEGG Orthology-Based Annotation System, intelligent version (KOBAS-i) (Bu et al., 2021). The *Mizuhopecten yessoensis* bivalve mollusk was used as reference species for the KEGG pathway enrichment analysis. For both GO terms and KEGG pathway enrichment analysis, an enrichment ratio was calculated as follows: Enrich ratio = Log10(observed/expected). This was the ratio between: i) the number of proteins in the network annotated with a given term, and ii) the number of proteins expected to be annotated with this term in a random network of the same size. Enrichment ratios > 1 with an adjusted p-value < 0.05 (FDR; Benjamini-Hochberg) were considered relevant.

2.5. Metabolomics and proteogenomics data fusion

A detailed description of this mid-level data fusion strategy was described in Dumas et al. (2022a). Briefly, variables of the different blocks (i.e. dataset named MetaboESI+, MetaboESI- and Proteo) were scaled to unit variance. MCUVE-PLS (Cai et al., 2008) and consensus OPLS-DA (Boccard and Rutledge, 2013) models were computed with combinations of toolboxes and in-house functions in the MATLAB® 8 environment (The MathWorks, Natick, USA). MCUVE-PLS was carried out on the three blocks using the libPLS 1.98 package (Li et al., 2018) from a population of 10^4 models with a calibration sample to total sample ratio of 0.7. A reliability index threshold of 2 was applied to remove variables considered uninformative and then reduce the dimensionality of the three blocks. Consensus OPLS-DA was then implemented using the K-OPLS package (Bylesjö et al., 2008) for fusion of the remaining data subsets, while comparing the solvent control (SC) to each exposure condition separately, i.e. low concentration 0.1 µg/L (SCvsLD) and high concentration 10 µg/L (SCvsHD). Both models were found to be optimal with two components (one predictive and one orthogonal) using leave-one-out cross-validation. The variable loadings provided by each consensus OPLS-DA model were then displayed on a shared and unique structures (SUS) plot to differentiate variables with common or specific patterns of variation between both exposure conditions. Thresholds were set to select the extreme variables of the SUS-plot, i.e. considered to be the most informative to explain the effects of the CBZ-DCF-VLF mixture at both concentrations on the protein and metabolite modulation. This variable selection strategy is expected to highlight correlated signatures of metabolites and proteins with potential biological significances.

3. Results

3.1. Performance of metabolomics, proteomics and data integration

The metabolic fingerprints consisted of 2,660 features in ESI- and 3,821 features in ESI+. The quality of the LC-HRMS acquisitions was validated as 77% of the features had a good analytical repeatability in both ESI modes across QC replicates (RSD < 30%). The datasets were then filtered for

subsequent processing (removal of isotopes and features with an RSD < 30% or a retention time outside relevant MS analysis period, e.g. <60 s or >1,250 s), resulting in 1,590 features in ESI- and 1,999 in ESI+.

The shotgun proteomics analysis generated 1,067,776 peptide spectra matches with a p-value of 0.05 or lower from the 2,061,124 recorded spectra (on average 52% of spectra interpreted). A total of 4,558 proteins were identified. Proteins that accumulated less than 30 spectral counts among all samples were filtered out, thereby resulting in a total of 3,079 proteins.

Regarding consensus OPLS-DA models, the SCvsLD model resulted in R2Y = 0.988 and Q2Y = 0.826 (Figure 1B), while the SCvsHD model gave R2Y = 0.983 and Q2Y = 0.906 (Figure 1C), indicating that each model explained > 98% of the data variability and had a predictive performance of > 82%.

Hence, variables were selected on the SUS-plot and included subsets of 232, 149 and 445 variables from the MetaboESI+, MetaboESI- and Proteo blocks, respectively (Figure 1A).

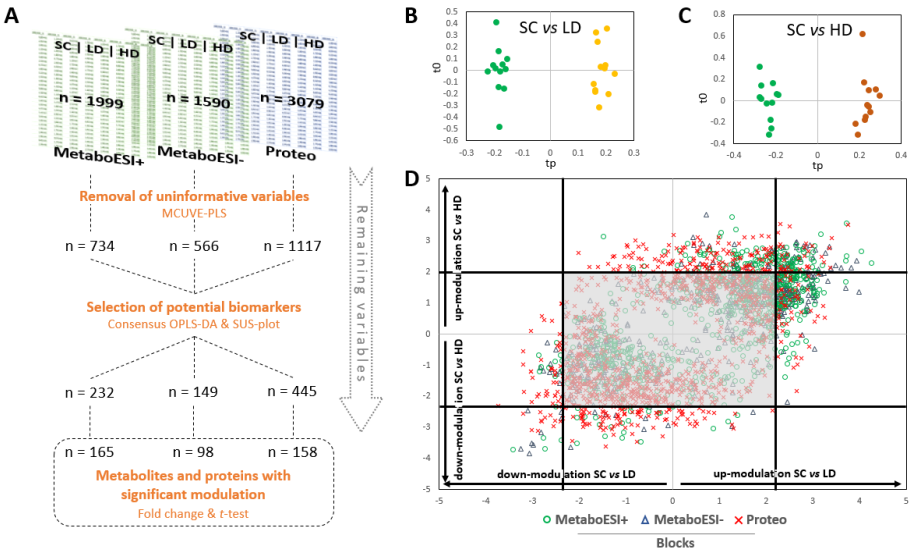

Figure 1: *Mid-level data fusion strategy based on MCUVE-PLS and consensus OPLS-DA analyses from the respective MetaboESI+, MetaboESI- and Proteo blocks.* ***(A)*** *The remaining variables from each block after each processing step. Score plots of the two consensus OPLS models with one orthogonal component (to) and one predictive component (tp):* ***(B)*** *solvent control exposure versus the low exposure concentration (SCvsLD) and* ***(C)*** *solvent control versus the high concentration (SCvsHD).* ***(D)*** *Shared and unique structures (SUS) plot integrating both SCvsLD and SCvsHD comparisons with common and specific modulations. Variables with a blue triangle belong to the MetaboESI+ block, those with a green circle to the*

MetaboESI- block and those with a red cross to the Proteo block. Thresholds are represented with black lines and less relevant variables are shaded.

The identification efforts were made on the variables selected by the consensus OPLS-DA models. Among these selected variables, 30 metabolites were annotated from the MetaboESI+ block, 31 metabolites from the MetaboESI- block and 343 proteins from the Proteo block. The metabolite and protein annotations are provided in Tables S1 and S2, respectively. Differential analysis of the abundance of annotated metabolites and proteins for both SC*vs*LD and SC*vs*HD comparisons (modulation amplitude and p-value) are given in Tables S1 and S2. Information on metabolites such as metabolic pathway, RSD QC, mass error, retention time, etc., are also available in Table S1.

The Venn diagrams provided the number of metabolites or proteins significantly modulated in a common or specific way depending on the exposure conditions (SC*vs*LD or SC*vs*HD) (Figure 2). Overall, greater effects on the metabolome and proteome of male mussels were observed for the high exposure concentration. Moreover, metabolites were more sensitive than proteins in revealing molecular changes triggered by the low exposure concentration.

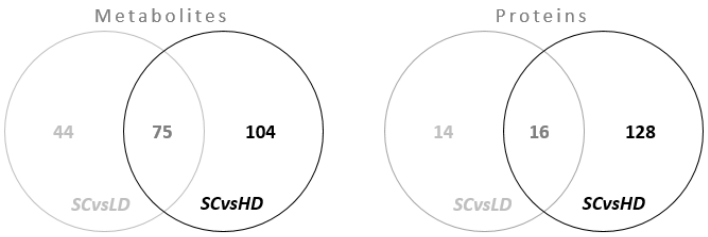

Figure 2: *Venn diagrams highlighting specific and common modulations of metabolites or proteins when comparing solvent control exposure versus low concentration exposure (SCvsLD), and solvent control versus high concentration (SCvsHD). Results are given for the selected variables according to the SUS plot.*

3.2. Mixture effects on proteome and metabolome

At the proteome level, the most significantly enriched KEGG pathways (Figure 3) were mainly related to carbohydrate, lipid, nucleotide and amino acid metabolisms, as well as protein synthesis and degradation processes. While only few of these pathways had an enrichment ratio of > 1 for the SC*vs*LD

399 condition (Figure 3A; n=7), more significantly enriched pathways were noted for the SC*vs*HD condition
400 (Figure 3B; n=14). Regarding GO term enrichment analysis, the results for both exposure conditions
401 (SC*vs*LD and SC*vs*HD) were categorized according to the biological process (Figure S1), molecular
402 function (Figure S2) and cellular component (Figure S3). Overall, these results corroborated those of
403 the KEGG pathway enrichment analysis and are presented in the Supplementary Data.

404 At the metabolome level, the modulated metabolites were mainly related to carbohydrate,
405 lipid, nucleotide and amino acid metabolisms, as well as cofactors and vitamins (Figure 4). Pathway
406 analysis revealed two significantly enriched metabolic pathways at both exposure concentrations,
407 including purine, nicotinate and nicotinamide metabolisms (Figure S4).

408 When considering both proteome and metabolome levels, consistent changes in protein and
409 metabolite abundances were observed, as outlined in the following sub-sections.

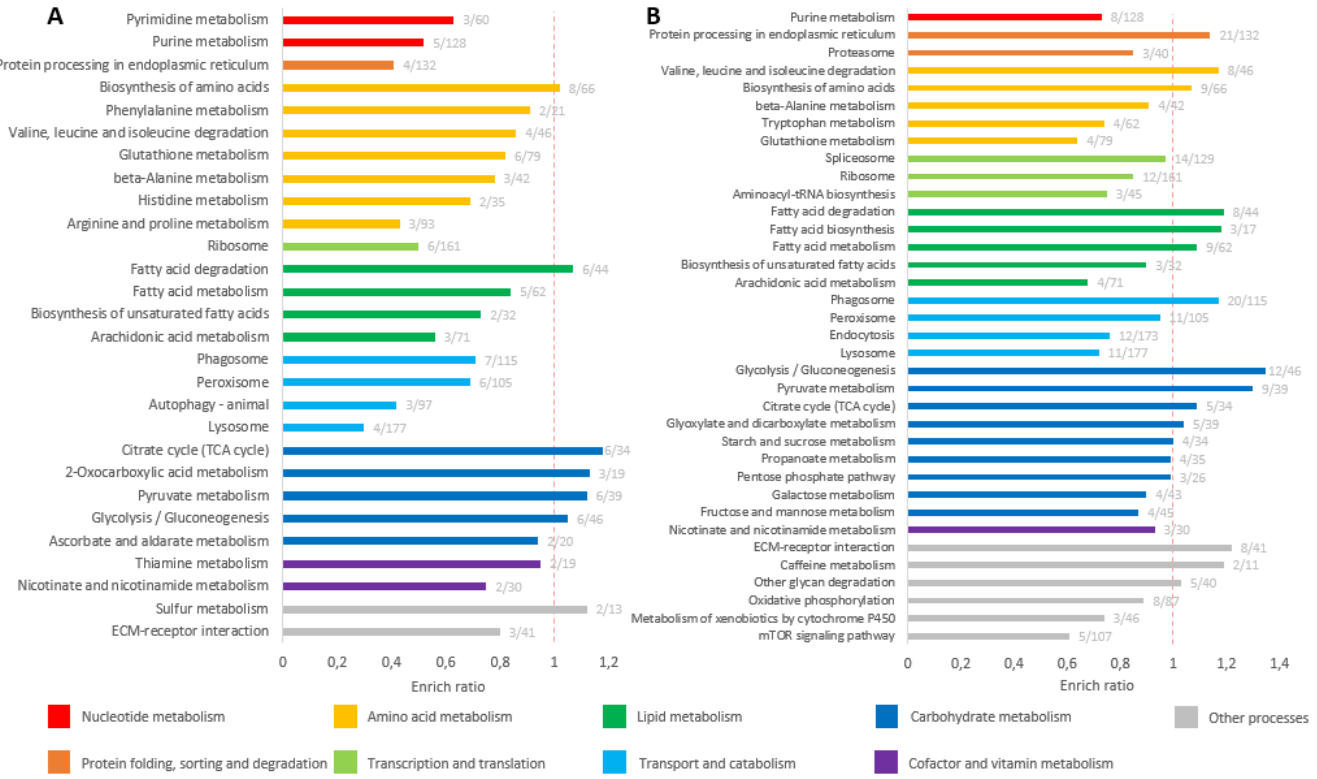

Figure 3: *KEGG pathway enrichment analysis with proteins selected via consensus OPLS-DA models, while considering* ***(A)*** *the low exposure concentration (0.1 µg/L; SCvsLD) or* ***(B)*** *the high exposure concentration (10 µg/L; SCvsHD). The label on each bar corresponds to the number of selected proteins associated with the pathway relative to the total number of proteins in that pathway.*

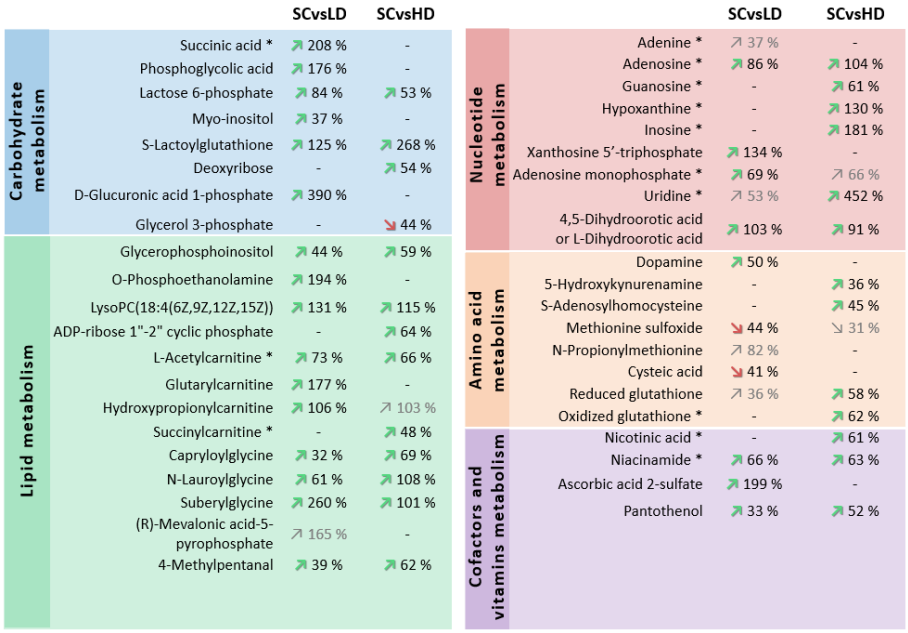

***Figure 4**: Main metabolites significantly up- or down-modulated by the low exposure concentration (SCvsLD) or the high exposure concentration (SCvsHD). Values in grey correspond to the modulation trend ($p < 0.1$). Asterisks indicate metabolites identified at level 1.*

3.2.1. Carbohydrate metabolism

Among the carbohydrate metabolism, citrate cycle (TCA cycle), glycolysis and pyruvate metabolism were interconnected pathways geared primarily towards producing energy (Figure 5). Glycolysis converged with the TCA cycle by providing phosphoenol pyruvate and then pyruvate. A slight up-modulation of four enzymes responsible for glucose conversion to phosphoenol pyruvate was observed under the SCvsHD condition (Figure 5, Table S2). In addition, significant modulations in pyruvate kinase and pyruvate dehydrogenase E1 component subunit beta were highlighted at both exposure concentrations (Figure 5, Table S2). These two enzymes are involved in the conversion of phosphoenol pyruvate to pyruvate and then to acetyl-CoA, respectively, although these metabolites were not detected in this study. Acetyl-CoA was involved as a substrate in the TCA cycle. Changes in the TCA cycle were characterized by up-modulation of malate dehydrogenase and isocitrate

dehydrogenase [NAD] subunit gamma enzymes (Figure 5, Table S2), as well as the succinate metabolite (Figures 4 and 5).

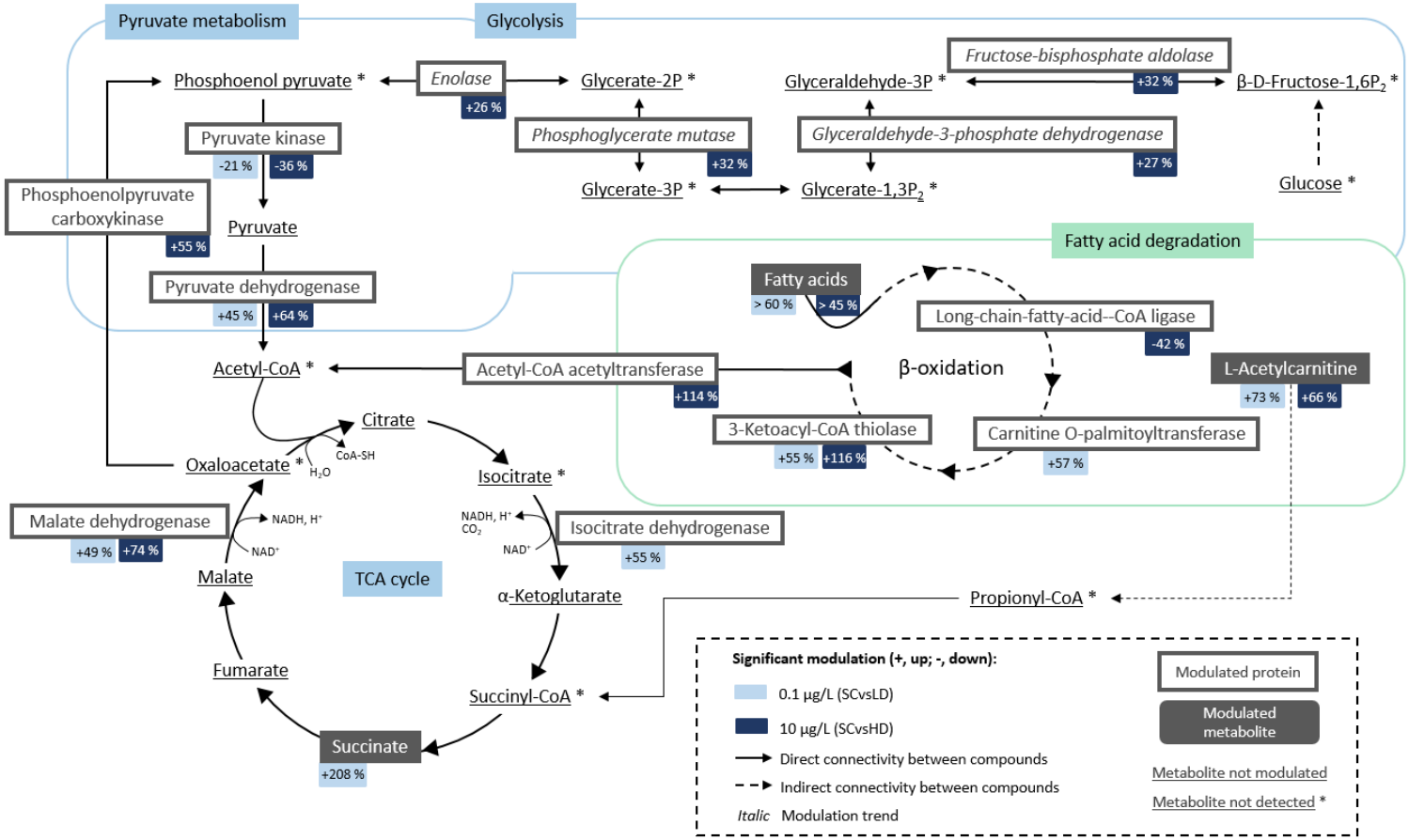

431

432 ***Figure 5:*** *Metabolic pathways of carbohydrate and lipid metabolism mapping proteins and metabolites modulated at low (SCvsLD) and high (SCvsHD) mixture exposure concentration.*

3.2.2. Lipid metabolism

Among the lipid metabolism, fatty acid degradation through β-oxidation in mitochondria was the main enriched pathway (Figure 3). Fatty acid degradation was also involved in energy production by providing acetyl-CoA to the TCA cycle (Figure 5). Modulation of three enzymes responsible for β-oxidation of fatty acids was observed (Figure 5, Table S2), along with up-modulation of acetyl-CoA acetyltransferase 1, which catalyzed the last step in the transformation of fatty acids into acetyl-CoA. Note that acetyl-CoA acetyltransferase was involved in other metabolic pathways, particularly in pyruvate metabolism and amino acid metabolism e.g., valine, leucine and isoleucine degradation, lysine degradation, as well as tryptophan metabolism.

Several metabolites associated with fatty acid metabolism were up-modulated at both exposure concentrations. Among them, four acylcarnitine compounds, including L-acetylcarnitine, were involved in energy production in mitochondria through beta-oxidation of fatty acids. In addition, three acylglycine compounds considered to be fatty acid oxidation metabolites were up-modulated (Figure 4, Table S1). L-acetylcarnitine plays an important role in the metabolism of both carbohydrates and lipids, leading to an increase in ATP generation. L-acetylcarnitine is transported to the mitochondria where it is transformed into free carnitine (detected but not modulated) and propionyl-CoA (not detected). The latter is converted into succinyl-CoA (not detected) and finally to succinic acid, which is involved in the TCA cycle. Consequently, the TCA cycle activity was enhanced, as highlighted by the high modulation of succinic acid and two other enzymes (Figures 4 and 5).

3.2.3. Nucleotide metabolism

Among nucleotide metabolism, purine metabolism was highly affected, with four up-modulated metabolites noted at the SC*vs*LD concentration and five up-modulated metabolites at the SCvsHD concentration (Figure 6, Table S1). Modulation of these metabolites was in accordance with proteomics results. Indeed, three proteins catalyzing metabolic reactions of these metabolites were

modulated in addition to adenosine deaminase (SC*vs*HD: +51%; $p < 0.01$; not selected by the models) (Figure 6).

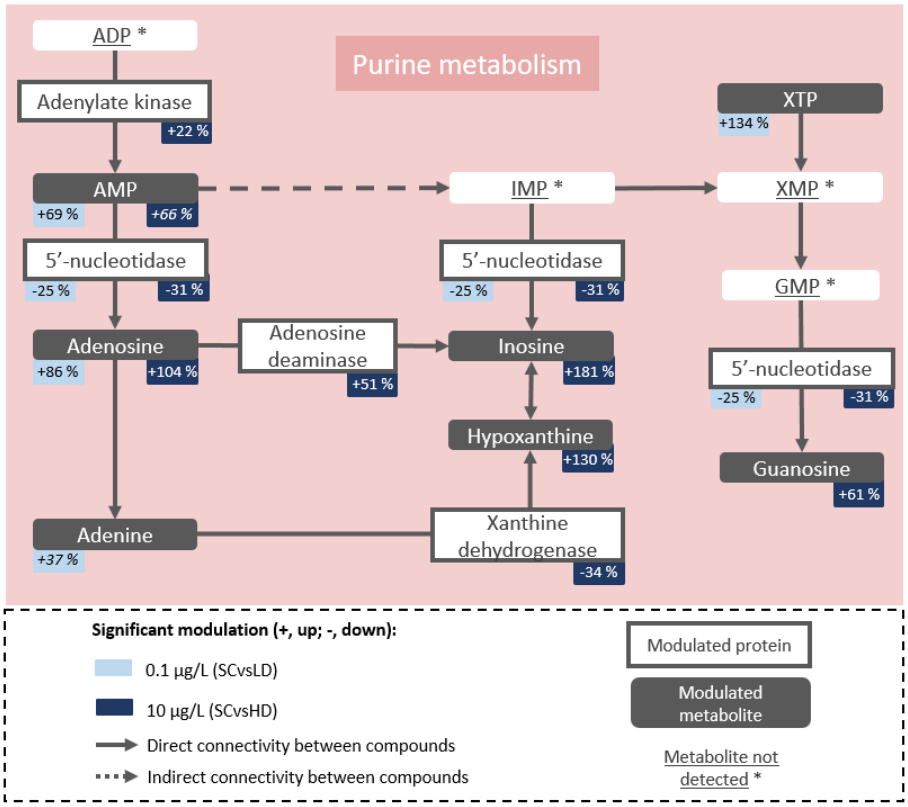

Figure 6: *Metabolic pathway of purine metabolism represented by consistent modulations of metabolite and protein abundance in the digestive gland of* Mytilus galloprovincialis *male mussels exposed at the low (SCvsLD; 0.1 µg/L) or high (SCvsHD; 10 µg/L) exposure concentration. ADP: adenosine 5'-diphosphate; AMP: adenosine monophosphate; IMP: inosine monophosphate; XMP: xanthosine 5'-phosphate; XTP: xanthosine 5'-triphosphate.*

3.2.4. Amino acid metabolism

Amino acid metabolism was mainly characterized by the disturbance of four metabolites from cysteine and methionine metabolism (Figure 4, Table S1). Down-modulation of methionine sulfoxide was consistent with the up-modulation of peptide methionine sulfoxide reductase MsrA (SC*vs*HD: +75%; $p < 0.01$) which catalyzes the reduction of protein-bound methionine sulfoxide back to methionine, although MsrA was not selected by the models.

469 Glutathione metabolism had an enrichment ratio < 1 (Figure 3), yet up-modulation of
470 glutathione peroxidase catalyzing the oxidation of glutathione (reduced state; GSH) into glutathione
471 disulfide (oxidized glutathione; GSSG) was measured at the two exposure concentrations (Table S2).
472 GSSG was up-modulated, in agreement with the proteomic results (Figure 4, Table S1). While down-
473 modulation of GSH would be expected in this case, its up-modulation could indicate GSH *de novo*
474 synthesis. However, caution is needed in interpreting this result as GSH was annotated at level 2.
475 Modulation of GSSG and GSH could also be related to up-modulation of glutathione S-transferase
476 sigma 1 (Table S2), which allows GSH conjugation to endogenous substrates or xenobiotics.

477 *3.2.5. Cofactors and vitamin metabolism*

478 Regarding vitamin metabolism, nicotinate and nicotinamide metabolism was the most
479 enriched pathway (Figure S4). Nicotinic acid, i.e. known as vitamin B3, was up-modulated at the high
480 exposure concentration, while niacinamide was up-modulated to the same extent at both exposure
481 concentrations (Figure 4, Table S1). Nicotinic acid and niacinamide are precursors of the coenzymes
482 nicotinamide-adenine dinucleotide (NAD+) and nicotinamide-adenine dinucleotide phosphate
483 (NADP+). These coenzymes are involved in a myriad of metabolic processes, including energy
484 metabolism, mitochondrial functions, calcium homeostasis, antioxidation/generation of oxidative
485 stress, gene expression, immunological functions and cell death.

486 *3.2.6. Protein synthesis and degradation processes*

487 Upstream of protein synthesis, modulations were first observed at the transcription
488 (spliceosome) and translation (ribosome, aminoacyl-tRNA biosynthesis) levels, mainly under the
489 SC*vs*HD condition (Figure 3, Table S2). From spliceosome, splicing factor, arginine/serine-rich 4 was up-
490 modulated while splicing factor 3B subunit 3 was down-modulated (Table S2). Ribosomal proteins such
491 as 40S ribosomal protein S6 was up-modulated and four other ribosomal proteins were modulated to
492 a lesser extent. In addition, four proteins involved in aminoacyl-tRNA biosynthesis were up-modulated,
493 including glycine-tRNA ligase and cysteine-tRNA ligase (Table S2), as well as tryptophan-tRNA ligase

494 (+43%; $p < 0.05$) and leucine-tRNA ligase (+91%; $p < 0.005$) which were not selected by the models.
495 The cellular machinery is thus remodeled for specific protein synthesis in response to stress.

496 A high number of proteins (n = 21) selected by the SC*vs*HD model were related to protein
497 processing in the endoplasmic reticulum (ER). These modulated proteins are involved in the folding
498 and sorting of newly synthetized proteins. Among them, significant modulation of the ERGIC-53
499 protein, ribosome-binding protein 1 and B-cell receptor-associated protein 31 was observed, while
500 lower modulation was noted for DnaJ homolog subfamily A member 1, endoplasmic reticulum
501 chaperone BiP, HSP 70.3, protein disulfide isomerase and protein disulfide isomerase family A member
502 6 (Table S2). Accumulation of misfolded and unfolded proteins can induce ER stress. To re-establish
503 the ER function and restore homeostasis, degradation pathways are activated, such as the ER-
504 associated protein degradation (ERAD) pathway or the unfolded protein response (UPR) signalling
505 pathway. In this study, significant up-modulation occurred for RuvB-like 2 from the ERAD pathway, and
506 DnaJ homolog subfamily C member 3 from the UPR signalling pathway (Table S2). Hence, protein
507 synthesis seemed to increase in response to the high exposure concentration, as well as ER stress
508 induced by the accumulation and degradation of unfolded and misfolded proteins.

3.3. Targeting the molecular signatures of CBZ, DCF and VLF

In this section we discuss the nature of the molecular effects, while questioning whether they resulted from interactive or additive effects. We hypothesized that if there is no interactive effect then we should observe an addition of molecular signatures similar to those reported under individual exposure conditions in previous studies. Inversely, interactions between the PhACs should lead to molecular signatures different from those obtained previously with individual exposure.

In order to target specific molecular signatures, we reviewed the literature on molecular effects triggered by single exposure of aquatic organisms to CBZ, DCF or VLF involving omics approaches (metabolomics, proteomics and transcriptomics). We found 15 articles, 5 of which were related to CBZ, 6 to DCF and 4 to VLF, including our previous publications focused on these three PhACs individually. Among these studies, 6 were conducted on molluscs, 6 on fish, 2 on crustacean and 1 on ascidian. The effects reported are described in Table S3, including modulated metabolites, proteins or transcripts, the most enriched metabolic pathways, GO terms and KO. Based on these reviewed data and the results obtained in this study, we have proposed an overview of common molecular effects as well as common enriched GO terms and KO (Table 1). Hence, the reported proteins, metabolites, GO terms and KO in Table 1 could correspond to the signature of CBZ, DCF or VLF within the observed mixture effects. Proteins, metabolites, GO terms and KO that were only observed for one of the pharmaceuticals, as highlighted in bold in Table 1 could therefore be considered as a specific signature of this PhAC in the mixture. For instance, the molecular signature of CBZ consisted of 21 proteins and 1 metabolite that had been modulated in previous studies with CBZ alone and with the mixture in the present study. Among these 21 proteins, 16 proteins (in bold) were only observed for CBZ (not modulated in previous studies for DCF and VLF exposures) and could thus be considered as a specific signature of CBZ effects in the mixture. In terms of GO and KO, the ER unfolded protein response, protein synthesis and degradation, and binding processes seemed to be specific to the CBZ signature. The molecular signature of DCF had the highest number of metabolites (n = 7) modulated by exposure

534 to the mixture. However, no specific signature of GO terms and KO was assigned to DCF. Regarding the
535 VLF signature, only a few proteins and metabolites (3 and 2, respectively) were specific, while changes
536 in glutathione metabolism and valine, leucine and isoleucine degradation seemed to be a specific
537 response of VLF in the mixture.

538 Hence, a moderate part of the observed modulations (32 proteins and 10 metabolites)
539 corresponded to the known molecular signatures of these three PhACs (Table 1) and may have resulted
540 from an additive effect. Furthermore, a major part of the modulated proteins and metabolites (Table
541 S1 and S2) had not been reported in previous exposures to PhAC alone. However, these proteins and
542 metabolites were mostly involved in the KO and GO terms already modulated by individual exposure
543 (Table 1). The response to these three PhACs will be discussed in the following section, while taking
544 their known MeOAs into account.

Table 1: *Signature of carbamazepine, diclofenac and venlafaxine observed in both single exposure conditions from the literature and under the current mixture exposure conditions. Bold annotations correspond to proteins/transcripts, metabolites or GO terms and KO specific to one of the three pharmaceuticals. Metabolites that tended to be modulated are in italics*

Contaminant	Signature of proteins or transcripts	Signature of metabolites	Signature of GO terms and KO	References
Carbamazepine (CBZ)	**40S ribosomal protein S6; ATP synthase subunit beta, mitochondrial;** Calmodulin; Cartilage matrix protein; Cathepsin L; Cathepsin L1; **Carboxypeptidase B; Coatomer subunit beta'; Dolichyl-diphosphooligosaccharide--protein glycosyltransferase subunit STT3B; Glutathione S-transferase sigma 1; Glycogen debranching enzyme; Histone H2A; Inositol-1-monophosphatase; Lachesin; Myophilin; Myosin VIIA; Protein ERGIC-53; RuvB-like 2; Thioredoxin-2; TNF ligand-like 1;** Tubulin alpha chain	Adenosine	Acyl carnitine compounds; Cysteine and methionine metabolism; **Endoplasmic reticulum unfolded protein response**; Fatty acid oxidation; **Metal ion binding**; **Nucleic acid binding**; Phenylalanine metabolism; Protein folding; **Protein synthesis and degradation**; Purine metabolism; TCA cycle	Baratange et al 2022; Dumas et al 2022; Navon et al 2021; Yan et al 2018; Kovacevic et al 2016
Diclofenac (DCF)	**ATP synthase subunits region ORF 7-like**; Calmodulin; Cartilage matrix protein; Cathepsin L; Cathepsin L1; **Cysteine--tRNA ligase, cytoplasmic; CD109; Dual oxidase 2; Glyceraldehyde-3-phosphate dehydrogenase; Malate dehydrogenase; Tryptophan--tRNA ligase, cytoplasmic;** Tubulin alpha-1A chain	**Acetylcarnitine**; ***Adenine***; **Hypoxanthine; Inosine; Niacinamide; Nicotinic acid; Uridine**	Acyl carnitine compounds; β-oxidation of very long chain fatty acids; Folding protein; Glucose metabolism; Nicotinate and nicotinamide metabolism; Pentose phosphate pathway; Phenylalanine metabolism; Purine metabolism; Pyrimidine metabolism; TCA cycle; Tryptophan metabolism; Tyrosine metabolism	Bonnefille et al 2018; Bouly et al 2022; Fu et al 2021; Schmidt et al 2013
Venlafaxine (VLF)	**Histidine ammonia-lyase; Phosphoenolpyruvate carboxykinase, cytosolic [GTP]; Serine--pyruvate aminotransferase**	Adenosine; **Deoxyribose; *N-Acetylvaline***	Cysteine and methionine metabolism; Glucose metabolism; **Glutathione metabolism**; Lipid metabolism; Nicotinate and nicotinamide metabolism; Pentose phosphate pathway; Phenylalanine metabolism; Purine metabolism; Pyrimidine metabolism; Tryptophan metabolism; Tyrosine metabolism; **Valine, leucine and isoleucine degradation**	Hong et al 2022; Ramirez et al 2022; Costa et al 2021; Best et al 2014

.

4. Discussion

A combined metabolomics and proteogenomics approach revealed molecular changes in digestive gland of male mussels (*Mytilus galloprovincialis*) exposed for 7 days to the CBZ-DCF-VLF mixture at low and high concentration. Consistent observed proteome and metabolome changes were the result of combined omics analyses carried out on the same samples (digestive glands), as well as of a mid-level data fusion strategy, that led to the selection of correlated protein and metabolite signatures. According to current knowledge, some of these statistically correlated signatures appear to be biologically relevant. As discussed below, those changes are mainly related to energy metabolism, protein synthesis, ER stress, defense mechanisms and oxidative stress. The known MeOAs of CBZ (e.g. cAMP depletion, GABA receptor agonist, voltage-dependent Na^+ and K^+ channels interaction, autophagy induction), DCF (e.g. cyclooxygenases inhibition and prostaglandins depletion) and VLF (e.g. serotonin increase) were taken into consideration to gain insight into the mixture effects.

4.1. Energy metabolism and fatty acid oxidation

Overall, exposure to the CBZ-DCF-VLF mixture triggered a major energy metabolism response. The TCA cycle, glycolysis, pyruvate metabolism and fatty acid degradation are interconnected pathways whose ultimate goal is primarily to produce energy such as ATP. Such results are not surprising as the digestive gland of bivalves plays an important role in the storage of metabolic reserves, thereby providing energy during stress periods (Gosling, 2015). The increased energy demand caused by contaminant exposure is a common metabolic response to detoxify the organism, maintain cellular homeostasis and repair damage. For instance, depletion of energy reserves (lipid, glycogen and protein) has been measured in digestive glands of *M. galloprovincialis* following 11 weeks exposure to 1.2 µg/L of the hypolipidemic drug atorvastatin (Falfushynska et al., 2019). Regarding the pharmaceutical mixture tested in the present study, single exposure to CBZ, DCF or VLF have already been found to disturb energy metabolism in aquatic organisms. In our previous study, exposure of male mussels (*M. galloprovincialis*) to CBZ (0.08 and 8 µg/L; 3 days) led to the disruption of fatty acid

degradation in mitochondria and peroxisomes through the modulation of several enzymes involved in fatty acid β-oxidation, as well as many fatty acids, acylcarnitines and acylglycines (Dumas et al., 2022a). In the same way, DCF was also shown to alter fatty acid β-oxidation in various aquatic organisms (Bouly et al., 2021; Fu et al., 2021). Fu et al. (2021) observed a modulation of several acylcarnitines in the *Hyalella azteca* crustacean exposed to DCF (10 and 100 µg/L) for 10 days, revealing a perturbation in the carnitine shuttle. The carnitine shuttle is a critical process for the transport of long-chain fatty acids from cell plasma across the membrane to mitochondria subsequent to β-oxidation. Furthermore, L-carnitine and L-acetylcarnitine were modulated in the *Lymnaea stagnalis* gastropod exposed for 16 weeks post-hatch to 0.1 µg/L of DCF (Bouly et al., 2021). While VLF does not disrupt fatty acid β-oxidation, it was reported to induce changes in transcript expression related to lipid metabolism, glucose metabolism and energy metabolism measured in the marine fish *Dicentrarchrus labrax* following 21 days exposure at 0.01 and 1 µg/L concentration (Costa et al., 2021). The combined effects of these three PhACs on energy metabolism were thus conserved, although such effects could be considered as a general response to cope with stress, and were not necessarily related to their expected MeOAs.

4.2. Protein synthesis and endoplasmic reticulum stress

Exposure to the CBZ-DCF-VLF mixture also triggered an intensification of processes related to protein synthesis, with subsequent ER stress induction, particularly at high concentration. Indeed, numerous modulated proteins are involved in transcription (spliceosome), translation (ribosome, aminoacyl-tRNA biosynthesis) and protein processing in ER (protein folding, sorting and degradation). When the demand for protein folding increases (e.g. enhanced protein synthesis, accumulation of mutated or abnormal proteins, etc.) and exceeds the protein folding capacity, misfolded/unfolded proteins accumulate in the ER lumen and trigger ER stress (Foufelle and Fromenty, 2016). Such stress has also been confirmed by activation of the unfolded protein response (UPR) through up-modulation of the DnaJ homolog subfamily C member 3. When CBZ exposure was found to cause ER stress in *M.*

598 *galloprovincialis* digestive glands (Dumas et al., 2022a), we argued that CBZ induced autophagy
599 through ER stress induction (e.g. accumulation of misfolded proteins, changes in calcium [Ca^{2+}] levels)
600 or inhibition of inositol monophosphatase, leading to free inositol depletion and reduced myo-inositol-
601 1,4,5-triphosphate. In this study, we observed both ER stress and down-modulation of inositol-1-
602 monophosphatase, although no proteins involved in autophagy were detected. These effects could
603 hence be related to the MeOA of CBZ. To our knowledge, ER stress induction caused by DCF or VLF in
604 aquatic organisms has not been previously reported. Otherwise, prolonged ER stress can affect the
605 organism's functions (protein synthesis and folding, lipid synthesis and Ca^{2+} homeostasis) and
606 definitely lead to cell death or apoptosis (Schwarz and Blower, 2016).

607 ### 4.3. Defense mechanisms and oxidative stress

608 The CBZ-DCF-VLF mixture also triggered defense mechanisms at both exposure
609 concentrations, including the biotransformation process and protection against oxidative stress.
610 Glutathione S-transferases (GSTs), which were up-modulated in this study, are a family of phase II
611 biotransformation enzymes, catalyzing conjugation of the reduced form of glutathione (GSH) to
612 xenobiotics. Some GST isoforms are also capable of neutralizing lipoperoxidation products through
613 GSH oxidation to GSSG (Regoli and Giuliani, 2014). *M. galloprovincialis* exposure to CBZ (0.1 µg/L; 7
614 days) and DCF (1 and 1000 µg/L; 96 h) have already been shown to increase GST activity in digestive
615 glands (Martin-Diaz et al., 2009; Schmidt et al., 2011), while there is no such data on VLF exposure in
616 molluscs. An increase in GST activity is nevertheless a common response of *M. galloprovincialis* during
617 PhACs exposure as shown in previous studies (Afsa et al., 2023; Capolupo et al., 2016; Freitas et al.,
618 2019). GSTs could also be involved in the formation of thiol metabolites resulting from the oxidation
619 of CBZ, whereby GSH would be conjugated to the carbonyl group of CBZ (Vernouillet et al., 2010).

620 Metabolism enhancement (e.g. protein synthesis, fatty acid degradation, energy metabolism,
621 etc.) induced an increase in aerobic reactions, leading to the accumulation of reactive oxygen species
622 (ROS), which can be toxic to cells. Regarding the antioxidant defense system, glutathione peroxidase

623 (GPx) plays major role by catalyzing the reduction of hydrogen peroxide, organic hydroperoxide and
624 lipid peroxides using GSH (Bhagat et al., 2016). In this study, up-modulation of GPx, as well as GSSG,
625 revealed oxidative stress induction at both exposure concentrations. Further evidence of oxidative
626 stress was highlighted in this study, as for instance the up-modulation of mitochondrial peroxiredoxin-
627 5. This thioredoxin peroxidase is an antioxidant enzyme known to have high affinity for organic
628 peroxides and peroxynitrite, and protect mitochondrial DNA from oxidative attack (Banmeyer et al.,
629 2005; De Simoni et al., 2013). ROS and reactive nitrogen intermediates can cause damage to many
630 cellular components such as proteins. In the latter, methionine is one of the most easily oxidized amino
631 acids, resulting in its conversion to methionine sulfoxide. As a repair mechanism, peptide methionine
632 sulfoxide reductase (MsrA) catalyzes the reduction of methionine sulfoxide, both free and protein-
633 bound, back to methionine, the lack of which would cause severe cellular damage (Weissbach et al.,
634 2002). This repair mechanism occurred in the digestive gland of male mussels exposed to the CBZ-DCF-
635 VLF mixture, as MsrA was up-modulated at high concentration, consistent with the down-modulation
636 of methionine sulfoxide. The fact that oxidative stress occurred in this experiment was not surprising
637 in the light of previous findings. Oxidative stress is the most common effect of CBZ reported in bivalves
638 (Almeida et al., 2020). Induction of oxidative stress has also been frequently reported for DCF, although
639 this process was more time-, concentration- and organism-dependent (Bonnefille et al., 2018a). In
640 vertebrates, VLF has a protective effect against oxidative stress due to its dual activity on the reuptake
641 inhibition of both serotonin and norepinephrine (Eren et al., 2007). This mechanism has been
642 confirmed in oyster immunocytes in which norepinephrine down-regulates interleukins, which are key
643 elements required for ROS production (Lacoste et al., 2001). Hence, the oxidative stress observed in
644 this study could mainly have been induced by CBZ and DCF, whereas to our knowledge VLF does not
645 induce oxidative stress in aquatic organisms.

646 The molecular response of mussels was also highly marked by changes in purine metabolism.
647 Nucleobases (e.g. adenine, hypoxanthine) are the building blocks for the synthesis of nucleosides (e.g.

adenosine, inosine, guanosine and uridine), which were up-modulated in this study. For instance, adenosine is well recognized as being part of ATP and ADP, which are crucial molecules in energy production. The addition of ribose and phosphate groups to the nucleobases generates nucleotides (e.g. AMP), which can be used in RNA synthesis, while the addition of deoxyribose (up-modulated in this study) leads to precursors which are used by the organism *in vivo* to synthesize DNA. Hence, the CBZ-DCF-VLF mixture could modify the turnover and repair mechanisms of genetic material. This hypothesis is also supported by the observed up-modulation of histone H2A (Table S2) leading to chromatin formation. Histones are subject to post-translational modifications which are intimately related to replication, recombination and DNA repair (Bergink et al., 2006). Hence, DNA damage through oxidative stress cannot be excluded.

Finally, the up-modulation of nicotinic acid and niacinamide (precursors of NAD+ and NADP+) was consistent with the proteomic and metabolomic results described in the discussion. NAD+ and NADP+ coenzymes are common fundamental mediators of various biological processes discussed in this study, including energy metabolism, mitochondrial functions, calcium homeostasis, antioxidant/oxidative stress induction and cell death (Ying, 2008). Interestingly, nicotinic acid and niacinamide modulation has been observed in *L. stagnalis* exposed to DCF (Bouly et al., 2021) and seems to be specific to the DCF molecular signature (Table 1). However, this modulation was not related to the known DCF MeOA, which is based on COX inhibition.

4.4. Contribution of omics to the study of mixture effects

By selecting a mixture of PhACs with different therapeutic classes that do not share known MeOAs, we initially hypothesized that if these PhACs do not interact in terms of molecular targets, then the resulting molecular signatures would be the sum of the already reported individual signatures of each PhAC. A possible limitation of this study to address such a question could be the lack of existing knowledge about molecular effects of these PhACs in bivalves. In addition, mixture effects are not strictly compared against individual exposures within the same study. Hence, comparison with

673 previous studies should be treated with caution due to differences in exposure conditions. Despite
674 these limitations, our study produces encouraging results for the continued use of multi-omics
675 approaches to investigate mixture effects.

676 Through our multi-omics approach, we observed similar effects of the CBZ-DCF-VLX mixture
677 compared to the effects induced by single exposure. Indeed, the molecular effects triggered by the
678 mixture, such as changes in energy metabolism and lipid metabolism, as well as oxidative stress
679 induction, increased protein synthesis and degradation followed by ER stress, have also been
680 previously reported for some or all of these three PhACs. Nevertheless, while certain effects of the
681 mixture could be linked to known individual effects of the PhACs, we did not detect any modulation
682 associated with the MeOA of DCF (e.g. cyclooxygenases and prostaglandins) or VLF (e.g. serotonin),
683 except for CBZ. This, however, should be carefully considered as many factors could explain why
684 modulations related to the MeOA were not observed (e.g. differences in exposure conditions, choice
685 of organisms and the absence of standardized methodology for omics). As described in the discussion,
686 ER stress induction and down-modulation of inositol monophosphatase could both be related to the
687 CBZ MeOA involved in autophagy induction. The stronger expression of the CBZ MeOA compared to
688 that of DCF and VLF may be related to the way CBZ is metabolized. Indeed, it is known that in human
689 CBZ can auto-induce its metabolization through the activation of hepatic cytochrome P450 (CYP)
690 enzymes (Ayano, 2016). Some CBZ metabolites such as carbamazepine-10,11-epoxide can also be
691 toxic, even more than CBZ (Heye et al., 2016). In addition, CYP induction by CBZ may also increase the
692 rate of metabolism of DCF or VLF. Indeed, CBZ can induce CYP3A4, CYP2C8 and CYP2C9 (Darwish et al.,
693 2015; Liu et al., 2015), which are also involved in DCF (Krasniqi et al., 2016) and VLF (Fogelman et al.,
694 1999) metabolization. Although CYP3A4 and CYP2C8 were detected in this study (results not shown),
695 no modulation was observed. Further research on the toxicokinetic interactions between these PhACs
696 is required to be able to further interpret these results.

Beyond potential toxicokinetic interactions, the overall molecular effects observed tended to support our initial hypothesis, suggesting that the mixture effects were predominantly additive. Our findings indicated that the multi-omics approach effectively identified the toxicity pathways associated with each individual molecule in the mixture, thereby showcasing the advantage of this molecular-based approach over apical-based endpoints for studying mixture effects. This advantage is particularly beneficial when the effects are additive, as the interpretation can be based on existing knowledge, which facilitates the detection of known effects or MeOAs. However, identifying interactive effects (e.g. synergistic or antagonistic) through omics approaches may be more challenging due to the complexity of the resulting molecular effects. To address this shortcoming, exposure to a mixture of PhACs belonging to the same therapeutic class and sharing similar MeOAs could potentially serve as training data for omics approaches to achieve more clear-cut detection of interactive effects. This could be further enhanced by exploring exposure to a mixture of PhACs with interactions known to trigger toxicity in humans. Such studies would also be very relevant to acknowledge effects on situations likely to occur in the environment.

Our findings also revealed that omics approaches are effective in detecting mixture effects, even at low concentrations. In fact, many of the effects observed at high concentration were also detected at the low exposure concentration. This highlights the relevance of omics in addressing environmental concerns as PhACs are commonly found at low concentration in the environment. Note also that the ecotoxicity of a mixture of PhACs could exceed the effects of individual compounds, even if each PhAC is present at a low concentration that would not individually cause significant toxicity to exposed organisms (Backhaus, 2014). In addition to binary or ternary mixtures, it is crucial to consider the realistic diversity of contaminants that occur in the environment in order to be able to fully understand the impact of anthropogenic discharges. Omics approaches have been applied in studies investigating the effects of environmental mixtures, such as wastewater treatment plant effluent, on aquatic organisms (Bebianno et al., 2016; Berlioz-Barbier et al., 2018; Dumas et al., 2020b, 2020a;

722 Simmons et al., 2017). These studies integrated the complexity of real-world mixture scenarios,
723 thereby providing a more comprehensive understanding of the potential mixture effects of
724 contaminants in the environment.

725 ## 5. Conclusion

726 Integration of metabolomics and proteogenomics approaches has proven to be very effective to
727 highlight consistent changes in metabolome and proteome of male mussels *Mytilus galloprovincialis*,
728 exposed 7 days to the CBZ-DCF-VLF mixture at a low and high concentration (0.1 and 10 µg/L). Such
729 consistent changes observed between the two molecular levels are the result of combined omics
730 analyses carried out on the same samples (digestive glands), as well as of a mid-level data fusion
731 strategy allowing the selection of correlated protein and metabolite signatures. Some of these
732 statistically correlated signatures have been shown to be biologically relevant, according to the current
733 knowledge. Such mixture-induced modulations of proteins and metabolites indicate a metabolic
734 disturbance, as well as endoplasmic reticulum stress and oxidative stress, even at the environmental
735 concentration, which can be damaging to marine bivalves under chronic exposure. The consideration
736 of the known MeOAs and molecular signatures of individual PhACs was essential to decipher the
737 mixture effects, thus revealing a potential additive effect. Finally, the present study clearly revealed
738 the ability of multi-omics to decipher MeOA in a non-target and non-model species, highlighting that
739 such promising approaches could help gain further insight into complex scenarios in relevant
740 environmental settings.

741 **Acknowledgement & Funding**

742 This research was funded by the French *Agence Nationale de la Recherche* (IMAP ANR-16-CE34-
743 0006-01). The post-doctoral research contract of Thibaut Dumas was financially supported by Sanofi
744 France. The authors thank the Platform of Non-Target Environmental Metabolomics (PONTEM) of the
745 Montpellier Alliance for Metabolomics and Metabolism Analysis (MAMMA) consortium facilities. The

technical assistance of Mélodie Kielbasa (Atomic Energy and Alternative Energies Commission, CEA, Bagnols-sur-Cèze, France) and proofreading assistance of David Manley are gratefully acknowledged.

Appendix A. Supporting information

Supplementary data associated with this article can be found in the online version.

6. References

Afsa, S., De Marco, G., Cristaldi, A., Giannetto, A., Galati, M., Billè, B., Oliveri Conti, G., ben Mansour, H., Ferrante, M., Cappello, T., 2023. Single and combined effects of caffeine and salicylic acid on mussel Mytilus galloprovincialis: Changes at histomorphological, molecular and biochemical levels. Environ. Toxicol. Pharmacol. 101, 104167. https://doi.org/10.1016/j.etap.2023.104167

Almeida, Â., Calisto, V., Esteves, V.I., Schneider, R.J., Soares, A.M.V.M., Freitas, R., 2022. Responses of Ruditapes philippinarum to contamination by pharmaceutical drugs under ocean acidification scenario. Sci. Total Environ. 824, 153591. https://doi.org/10.1016/j.scitotenv.2022.153591

Almeida, Â., Esteves, V.I., Soares, A.M.V.M., Freitas, R., 2020. Effects of Carbamazepine in Bivalves: A Review, in: Reviews of Environmental Contamination and Toxicology. Springer International Publishing, Cham, pp. 1–19. https://doi.org/10.1007/398_2020_51

Almeida, Â., Freitas, R., Calisto, V., Esteves, V.I., Schneider, R.J., Soares, A.M.V.M., Figueira, E., Campos, B., Barata, C., 2018. Effects of carbamazepine and cetirizine under an ocean acidification scenario on the biochemical and transcriptome responses of the clam Ruditapes philippinarum. Environ. Pollut. 235, 857–868. https://doi.org/10.1016/j.envpol.2017.12.121

Almeida, Â., Soares, A.M.V.M., Esteves, V.I., Freitas, R., 2021. Occurrence of the antiepileptic carbamazepine in water and bivalves from marine environments: A review. Environ. Toxicol. Pharmacol. 86, 103661. https://doi.org/10.1016/j.etap.2021.103661

Alvarez-Muñoz, D., Huerta, B., Fernandez-Tejedor, M., Rodríguez-Mozaz, S., Barceló, D., 2015. Multi-residue method for the analysis of pharmaceuticals and some of their metabolites in bivalves. Talanta 136, 174–182. https://doi.org/10.1016/j.talanta.2014.12.035

Ariza-Castro, N., Courant, F., Dumas, T., Marion, B., Fenet, H., Gomez, E., 2021. Elucidating venlafaxine metabolism in the Mediterranean mussel (Mytilus galloprovincialis) through combined targeted and non-targeted approaches. Sci. Total Environ. 779, 146387. https://doi.org/10.1016/j.scitotenv.2021.146387

Arpin-Pont, L., Bueno, M.J.M., Gomez, E., Fenet, H., 2016. Occurrence of PPCPs in the marine environment: a review. Environ. Sci. Pollut. Res. 23, 4978–4991. https://doi.org/10.1007/s11356-014-3617-x

Ayano, G., 2016. Bipolar Disorders and Carbamazepine: Pharmacokinetics,Pharmacodynamics, Therapeutic Effects and Indications of Carbamazepine: Review of Articles. Clin. Neuropsychol. Open Access 1, 1–5. https://doi.org/10.4172/2472-095X.1000112

Backhaus, T., 2014. Medicines, shaken and stirred: a critical review on the ecotoxicology of pharmaceutical mixtures. Philos. Trans. R. Soc. B Biol. Sci. 369, 20130585. https://doi.org/10.1098/rstb.2013.0585

Banmeyer, I., Marchand, C., Clippe, A., Knoops, B., 2005. Human mitochondrial peroxiredoxin 5 protects from mitochondrial DNA damages induced by hydrogen peroxide. FEBS Lett. 579, 2327–2333. https://doi.org/10.1016/j.febslet.2005.03.027

Bebianno, M.J., Sroda, S., Gomes, T., Chan, P., Bonnafe, E., Budzinski, H., Geret, F., 2016. Proteomic changes in Corbicula fluminea exposed to wastewater from a psychiatric hospital. Environ. Sci. Pollut. Res. 23, 5046–5055. https://doi.org/10.1007/s11356-015-5395-5

Benotti, M.J., Brownawell, B.J., 2009. Microbial degradation of pharmaceuticals in estuarine and coastal seawater. Environ. Pollut. 157, 994–1002. https://doi.org/10.1016/j.envpol.2008.10.009

Bergink, S., Salomons, F.A., Hoogstraten, D., Groothuis, T.A.M., Waard, H. de, Wu, J., Yuan, L., Citterio, E., Houtsmuller, A.B., Neefjes, J., Hoeijmakers, J.H.J., Vermeulen, W., Dantuma, N.P., 2006. DNA damage triggers nucleotide excision repair-dependent monoubiquitylation of histone H2A. Genes Dev. 20, 1343–1352. https://doi.org/10.1101/gad.373706

Berlioz-Barbier, A., Buleté, A., Fildier, A., Garric, J., Vulliet, E., 2018. Non-targeted investigation of benthic invertebrates (Chironomus riparius) exposed to wastewater treatment plant effluents using nanoliquid chromatography coupled to high-resolution mass spectrometry. Chemosphere 196, 347–353. https://doi.org/10.1016/j.chemosphere.2018.01.001

Bhagat, J., Ingole, B.S., Singh, N., 2016. Glutathione S-transferase, catalase, superoxide dismutase, glutathione peroxidase, and lipid peroxidation as biomarkers of oxidative stress in snails: A review. Invertebr. Surviv. J. 13, 336–349. https://doi.org/10.25431/1824-307X/isj.v13i1.336-349

Blaženović, I., Kind, T., Ji, J., Fiehn, O., 2018. Software Tools and Approaches for Compound Identification of LC-MS/MS Data in Metabolomics. Metabolites 8, 31. https://doi.org/10.3390/metabo8020031

Boccard, J., Rutledge, D.N., 2013. A consensus orthogonal partial least squares discriminant analysis (OPLS-DA) strategy for multiblock Omics data fusion. Anal. Chim. Acta 769, 30–39. https://doi.org/10.1016/j.aca.2013.01.022

Boillot, C., Martinez Bueno, M.J., Munaron, D., Le Dreau, M., Mathieu, O., David, A., Fenet, H., Casellas, C., Gomez, E., 2015. In vivo exposure of marine mussels to carbamazepine and 10-hydroxy-10,11-dihydro-carbamazepine: Bioconcentration and metabolization. Sci. Total Environ. 532, 564–570. https://doi.org/10.1016/j.scitotenv.2015.05.067

Bonnefille, B., Arpin-Pont, L., Gomez, E., Fenet, H., Courant, F., 2017. Metabolic profiling identification of metabolites formed in Mediterranean mussels (Mytilus galloprovincialis) after diclofenac exposure. Sci. Total Environ. 583, 257–268. https://doi.org/10.1016/j.scitotenv.2017.01.063

Bonnefille, B., Gomez, E., Alali, M., Rosain, D., Fenet, H., Courant, F., 2018a. Metabolomics assessment of the effects of diclofenac exposure on Mytilus galloprovincialis: Potential effects on osmoregulation and reproduction. Sci. Total Environ. 613–614, 611–618. https://doi.org/10.1016/j.scitotenv.2017.09.146

Bonnefille, B., Gomez, E., Courant, F., Escande, A., Fenet, H., 2018b. Diclofenac in the marine environment: A review of its occurrence and effects. Mar. Pollut. Bull. 131, 496–506. https://doi.org/10.1016/j.marpolbul.2018.04.053

Bouly, L., Courant, F., Bonnafé, E., Carayon, J.-L., Malgouyres, J.-M., Vignet, C., Gomez, E., Géret, F., Fenet, H., 2021. Long-term exposure to environmental diclofenac concentrations impairs growth and induces molecular changes in Lymnaea stagnalis freshwater snails. Chemosphere 133065. https://doi.org/10.1016/j.chemosphere.2021.133065

Branchet, P., Arpin-Pont, L., Piram, A., Boissery, P., Wong-Wah-Chung, P., Doumenq, P., 2021. Pharmaceuticals in the marine environment: What are the present challenges in their monitoring? Sci. Total Environ. 766, 142644. https://doi.org/10.1016/j.scitotenv.2020.142644

Bu, D., Luo, H., Huo, P., Wang, Z., Zhang, S., He, Z., Wu, Y., Zhao, L., Liu, J., Guo, J., Fang, S., Cao, W., Yi, L., Zhao, Y., Kong, L., 2021. KOBAS-i: intelligent prioritization and exploratory visualization of biological functions for gene enrichment analysis. Nucleic Acids Res. 49, W317–W325. https://doi.org/10.1093/nar/gkab447

Bylesjö, M., Rantalainen, M., Nicholson, J.K., Holmes, E., Trygg, J., 2008. K-OPLS package: Kernel-based orthogonal projections to latent structures for prediction and interpretation in feature space. BMC Bioinformatics 9, 106. https://doi.org/10.1186/1471-2105-9-106

842 Cai, W., Li, Y., Shao, X., 2008. A variable selection method based on uninformative variable
843 elimination for multivariate calibration of near-infrared spectra. Chemom. Intell. Lab. Syst.
844 90, 188–194. https://doi.org/10.1016/j.chemolab.2007.10.001
845 Calisto, V., Domingues, M.R.M., Erny, G.L., Esteves, V.I., 2011. Direct photodegradation of
846 carbamazepine followed by micellar electrokinetic chromatography and mass spectrometry.
847 Water Res. 45, 1095–1104. https://doi.org/10.1016/j.watres.2010.10.037
848 Capolupo, M., Valbonesi, P., Kiwan, A., Buratti, S., Franzellitti, S., Fabbri, E., 2016. Use of an
849 integrated biomarker-based strategy to evaluate physiological stress responses induced by
850 environmental concentrations of caffeine in the Mediterranean mussel Mytilus
851 galloprovincialis. Sci. Total Environ. 563–564, 538–548.
852 https://doi.org/10.1016/j.scitotenv.2016.04.125
853 Castaño-Ortiz, J.M., Courant, F., Gomez, E., García-Pimentel, M.M., León, V.M., Campillo, J.A., Santos,
854 L.H.M.L.M., Barceló, D., Rodríguez-Mozaz, S., 2023. Combined exposure of the bivalve
855 Mytilus galloprovincialis to polyethylene microplastics and two pharmaceuticals (citalopram
856 and bezafibrate): Bioaccumulation and metabolomic studies. J. Hazard. Mater. 458, 131904.
857 https://doi.org/10.1016/j.jhazmat.2023.131904
858 Chan, W.T., Medriano, C.A., Bae, S., 2023. Unveiling the impact of short-term polyethylene
859 microplastics exposure on metabolomics and gut microbiota in earthworms (Eudrilus
860 euganiae). J. Hazard. Mater. 460, 132305. https://doi.org/10.1016/j.jhazmat.2023.132305
861 Clara, M., Strenn, B., Kreuzinger, N., 2004. Carbamazepine as a possible anthropogenic marker in the
862 aquatic environment: investigations on the behaviour of Carbamazepine in wastewater
863 treatment and during groundwater infiltration. Water Res. 38, 947–954.
864 https://doi.org/10.1016/j.watres.2003.10.058
865 Cogne, Y., Degli-Esposti, D., Pible, O., Gouveia, D., François, A., Bouchez, O., Eché, C., Ford, A.,
866 Geffard, O., Armengaud, J., Chaumot, A., Almunia, C., 2019. De novo transcriptomes of 14
867 gammarid individuals for proteogenomic analysis of seven taxonomic groups. Sci. Data 6,
868 184. https://doi.org/10.1038/s41597-019-0192-5
869 Costa, C., Semedo, M., Machado, S.P., Cunha, V., Ferreira, M., Urbatzka, R., 2021. Transcriptional
870 analyses reveal different mechanism of toxicity for a chronic exposure to fluoxetine and
871 venlafaxine on the brain of the marine fish Dicentrarchrus labrax. Comp. Biochem. Physiol.
872 Part C Toxicol. Pharmacol. 250, 109170. https://doi.org/10.1016/j.cbpc.2021.109170
873 Courant, F., Arpin-Pont, L., Bonnefille, B., Vacher, S., Picot-Groz, M., Gomez, E., Fenet, H., 2017.
874 Exposure of marine mussels to diclofenac: modulation of prostaglandin biosynthesis.
875 Environ. Sci. Pollut. Res. 1–8. https://doi.org/10.1007/s11356-017-9228-6
876 Cunha, M., Silva, M.G., De Marchi, L., Morgado, R.G., Esteves, V.I., Meucci, V., Battaglia, F., Soares,
877 A.MVM., Pretti, C., Freitas, R., 2023. Toxic effects of a mixture of pharmaceuticals in Mytilus
878 galloprovincialis: The case of 17α-ethinylestradiol and salicylic acid. Environ. Pollut. 324,
879 121070. https://doi.org/10.1016/j.envpol.2023.121070
880 Darwish, M., Bond, M., Yang, R., Hellriegel, E.T., Robertson, P., 2015. Evaluation of the Potential for
881 Pharmacokinetic Drug–Drug Interaction Between Armodafinil and Carbamazepine in Healthy
882 Adults. Clin. Ther. 37, 325–337. https://doi.org/10.1016/j.clinthera.2014.09.014
883 De Marco, G., Billè, B., Brandão, F., Galati, M., Pereira, P., Cappello, T., Pacheco, M., 2023.
884 Differential Cell Metabolic Pathways in Gills and Liver of Fish (White Seabream Diplodus
885 sargus) Coping with Dietary Methylmercury Exposure. Toxics 11, 181.
886 https://doi.org/10.3390/toxics11020181
887 De Simoni, S., Linard, D., Hermans, E., Knoops, B., Goemaere, J., 2013. Mitochondrial peroxiredoxin-5
888 as potential modulator of mitochondria-ER crosstalk in MPP+-induced cell death. J.
889 Neurochem. 125, 473–485. https://doi.org/10.1111/jnc.12117
890 Desbiolles, F., Malleret, L., Tiliacos, C., Wong-Wah-Chung, P., Laffont-Schwob, I., 2018. Occurrence
891 and ecotoxicological assessment of pharmaceuticals: Is there a risk for the Mediterranean

aquatic environment? Sci. Total Environ. 639, 1334–1348. https://doi.org/10.1016/j.scitotenv.2018.04.351
Di Nica, V., Villa, S., Finizio, A., 2017. Toxicity of individual pharmaceuticals and their mixtures to Aliivibrio fischeri: Evidence of toxicological interactions in binary combinations. Environ. Toxicol. Chem. 36, 815–822. https://doi.org/10.1002/etc.3686
Dondero, F., Negri, A., Boatti, L., Marsano, F., Mignone, F., Viarengo, A., 2010. Transcriptomic and proteomic effects of a neonicotinoid insecticide mixture in the marine mussel (Mytilus galloprovincialis, Lam.). Sci. Total Environ., Cumulative Stressors - Risk assessment of mixtures of chemicals and combinations of chemicals and natural stressors 408, 3775–3786. https://doi.org/10.1016/j.scitotenv.2010.03.040
Dumas, T., Boccard, J., Gomez, E., Fenet, H., Courant, F., 2020a. Multifactorial Analysis of Environmental Metabolomic Data in Ecotoxicology: Wild Marine Mussel Exposed to WWTP Effluent as a Case Study. Metabolites 10, 269. https://doi.org/10.3390/metabo10070269
Dumas, T., Bonnefille, B., Gomez, E., Boccard, J., Castro, N.A., Fenet, H., Courant, F., 2020b. Metabolomics approach reveals disruption of metabolic pathways in the marine bivalve Mytilus galloprovincialis exposed to a WWTP effluent extract. Sci. Total Environ. 712, 136551. https://doi.org/10.1016/j.scitotenv.2020.136551
Dumas, T., Courant, F., Almunia, C., Boccard, J., Rosain, D., Duporté, G., Armengaud, J., Fenet, H., Gomez, E., 2022a. An integrated metabolomics and proteogenomics approach reveals molecular alterations following carbamazepine exposure in the male mussel Mytilus galloprovincialis. Chemosphere 286, 131793. https://doi.org/10.1016/j.chemosphere.2021.131793
Dumas, T., Courant, F., Fenet, H., Gomez, E., 2022b. Environmental Metabolomics Promises and Achievements in the Field of Aquatic Ecotoxicology: Viewed through the Pharmaceutical Lens. Metabolites 12, 186. https://doi.org/10.3390/metabo12020186
Eggen, R.I.L., Behra, R., Burkhardt-Holm, P., Escher, B.I., Schweigert, N., 2004. Peer Reviewed: Challenges in Ecotoxicology. Environ. Sci. Technol. 38, 58A-64A. https://doi.org/10.1021/es040349c
Eren, İ., Nazıroğlu, M., Demirdaş, A., Çelik, Ö., Uğuz, A.C., Altunbaşak, A., Özmen, İ., Uz, E., 2007. Venlafaxine Modulates Depression-Induced Oxidative Stress in Brain and Medulla of Rat. Neurochem. Res. 32, 497–505. https://doi.org/10.1007/s11064-006-9258-9
Fabbri, E., Franzellitti, S., 2016. Human pharmaceuticals in the marine environment: Focus on exposure and biological effects in animal species. Environ. Toxicol. Chem. 35, 799–812. https://doi.org/10.1002/etc.3131
Falfushynska, H., Sokolov, E.P., Haider, F., Oppermann, C., Kragl, U., Ruth, W., Stock, M., Glufke, S., Winkel, E.J., Sokolova, I.M., 2019. Effects of a common pharmaceutical, atorvastatin, on energy metabolism and detoxification mechanisms of a marine bivalve Mytilus edulis. Aquat. Toxicol. 208, 47–61. https://doi.org/10.1016/j.aquatox.2018.12.022
Fernández-Rubio, J., Rodríguez-Gil, J.L., Postigo, C., Mastroianni, N., López de Alda, M., Barceló, D., Valcárcel, Y., 2019. Psychoactive pharmaceuticals and illicit drugs in coastal waters of North-Western Spain: Environmental exposure and risk assessment. Chemosphere 224, 379–389. https://doi.org/10.1016/j.chemosphere.2019.02.041
Fogelman, S.M., Schmider, J., Venkatakrishnan, K., von Moltke, L.L., Harmatz, J.S., Shader, R.I., Greenblatt, D.J., 1999. O- and N-demethylation of Venlafaxine In Vitro by Human Liver Microsomes and by Microsomes from cDNA-Transfected Cells: Effect of Metabolic Inhibitors and SSRI Antidepressants. Neuropsychopharmacology 20, 480–490. https://doi.org/10.1016/S0893-133X(98)00113-4
Fong, P.P., Bury, T.B., Dworkin-Brodsky, A.D., Jasion, C.M., Kell, R.C., 2015. The antidepressants venlafaxine ("Effexor") and fluoxetine ("Prozac") produce different effects on locomotion in two species of marine snail, the oyster drill (Urosalpinx cinerea) and the starsnail (Lithopoma

942 americanum). Mar. Environ. Res. 103, 89–94.
943 https://doi.org/10.1016/j.marenvres.2014.11.010
944 Foufelle, F., Fromenty, B., 2016. Role of endoplasmic reticulum stress in drug-induced toxicity.
945 Pharmacol. Res. Perspect. 4, e00211. https://doi.org/10.1002/prp2.211
946 Freitas, R., Almeida, Â., Calisto, V., Velez, C., Moreira, A., Schneider, R.J., Esteves, V.I., Wrona, F.J.,
947 Figueira, E., Soares, A.M.V.M., 2016. The impacts of pharmaceutical drugs under ocean
948 acidification: New data on single and combined long-term effects of carbamazepine on
949 Scrobicularia plana. Sci. Total Environ. 541, 977–985.
950 https://doi.org/10.1016/j.scitotenv.2015.09.138
951 Freitas, R., Silvestro, S., Coppola, F., Meucci, V., Battaglia, F., Intorre, L., Soares, A.M.V.M., Pretti, C.,
952 Faggio, C., 2019. Biochemical and physiological responses induced in Mytilus galloprovincialis
953 after a chronic exposure to salicylic acid. Aquat. Toxicol. 214, 105258.
954 https://doi.org/10.1016/j.aquatox.2019.105258
955 Fu, Q., Scheidegger, A., Laczko, E., Hollender, J., 2021. Metabolomic Profiling and Toxicokinetics
956 Modeling to Assess the Effects of the Pharmaceutical Diclofenac in the Aquatic Invertebrate
957 Hyalella azteca. Environ. Sci. Technol. 55, 7920–7929.
958 https://doi.org/10.1021/acs.est.0c07887
959 Godoy, A.A., Kummrow, F., 2017. What do we know about the ecotoxicology of pharmaceutical and
960 personal care product mixtures? A critical review. Crit. Rev. Environ. Sci. Technol. 47, 1453–
961 1496. https://doi.org/10.1080/10643389.2017.1370991
962 Gomez, E., Boillot, C., Martinez Bueno, M.J., Munaron, D., Mathieu, O., Courant, F., Fenet, H., 2021.
963 In vivo exposure of marine mussels to venlafaxine: bioconcentration and metabolization.
964 Environ. Sci. Pollut. Res. 28, 68862–68870. https://doi.org/10.1007/s11356-021-14893-4
965 Gosling, E., 2015. Marine Bivalve Molluscs, 2nd ed. John Wiley & Sons, Chichester.
966 Haas, B.J., Papanicolaou, A., Yassour, M., Grabherr, M., Blood, P.D., Bowden, J., Couger, M.B., Eccles,
967 D., Li, B., Lieber, M., MacManes, M.D., Ott, M., Orvis, J., Pochet, N., Strozzi, F., Weeks, N.,
968 Westerman, R., William, T., Dewey, C.N., Henschel, R., LeDuc, R.D., Friedman, N., Regev, A.,
969 2013. De novo transcript sequence reconstruction from RNA-seq using the Trinity platform
970 for reference generation and analysis. Nat. Protoc. 8, 1494–1512.
971 https://doi.org/10.1038/nprot.2013.084
972 Hai, F.I., Yang, S., Asif, M.B., Sencadas, V., Shawkat, S., Sanderson-Smith, M., Gorman, J., Xu, Z.-Q.,
973 Yamamoto, K., 2018. Carbamazepine as a Possible Anthropogenic Marker in Water:
974 Occurrences, Toxicological Effects, Regulations and Removal by Wastewater Treatment
975 Technologies. Water 10, 107. https://doi.org/10.3390/w10020107
976 Hartmann, E.M., Allain, F., Gaillard, J.-C., Pible, O., Armengaud, J., 2014. Taking the Shortcut for High-
977 Throughput Shotgun Proteomic Analysis of Bacteria, in: Vergunst, A.C., O'Callaghan, D. (Eds.),
978 Host-Bacteria Interactions: Methods and Protocols, Methods in Molecular Biology. Springer,
979 New York, NY, pp. 275–285. https://doi.org/10.1007/978-1-4939-1261-2_16
980 Hayoun, K., Gouveia, D., Grenga, L., Pible, O., Armengaud, J., Alpha-Bazin, B., 2019. Evaluation of
981 Sample Preparation Methods for Fast Proteotyping of Microorganisms by Tandem Mass
982 Spectrometry. Front. Microbiol. 10, 1985. https://doi.org/10.3389/fmicb.2019.01985
983 Heye, K., Becker, D., Lütke Eversloh, C., Durmaz, V., Ternes, T.A., Oetken, M., Oehlmann, J., 2016.
984 Effects of carbamazepine and two of its metabolites on the non-biting midge Chironomus
985 riparius in a sediment full life cycle toxicity test. Water Res. 98, 19–27.
986 https://doi.org/10.1016/j.watres.2016.03.071
987 Kessner, D., Chambers, M., Burke, R., Agus, D., Mallick, P., 2008. ProteoWizard: open source software
988 for rapid proteomics tools development. Bioinformatics 24, 2534–2536.
989 https://doi.org/10.1093/bioinformatics/btn323
990 Kidd, K.A., Backhaus, T., Brodin, T., Inostroza, P.A., McCallum, E.S., 2023. Environmental Risks of
991 Pharmaceutical Mixtures in Aquatic Ecosystems: Reflections on a Decade of Research.
992 Environ. Toxicol. Chem. 00, 1–10. https://doi.org/10.1002/etc.5726

Klein, G., Mathé, C., Biola-Clier, M., Devineau, S., Drouineau, E., Hatem, E., Marichal, L., Alonso, B., Gaillard, J.-C., Lagniel, G., Armengaud, J., Carrière, M., Chédin, S., Boulard, Y., Pin, S., Renault, J.-P., Aude, J.-C., Labarre, J., 2016. RNA-binding proteins are a major target of silica nanoparticles in cell extracts. Nanotoxicology 10, 1555–1564. https://doi.org/10.1080/17435390.2016.1244299

Krasniqi, V., Dimovski, A., Domjanović, I.K., Bilić, I., Božina, N., 2016. How polymorphisms of the cytochrome P450 genes affect ibuprofen and diclofenac metabolism and toxicity. Arh. Hig. Rada Toksikol. 67, 1–8. https://doi.org/10.1515/aiht-2016-67-2754

Kuhl, C., Tautenhahn, R., Böttcher, C., Larson, T.R., Neumann, S., 2012. CAMERA: An Integrated Strategy for Compound Spectra Extraction and Annotation of Liquid Chromatography/Mass Spectrometry Data Sets. Anal. Chem. 84, 283–289. https://doi.org/10.1021/ac202450g

Labine, L.M., Pereira, E.A.O., Kleywegt, S., Jobst, K.J., Simpson, A.J., Simpson, M.J., 2023. Environmental metabolomics uncovers oxidative stress, amino acid dysregulation, and energy impairment in Daphnia magna with exposure to industrial effluents. Environ. Res. 234, 116512. https://doi.org/10.1016/j.envres.2023.116512

Lacaze, E., Pédelucq, J., Fortier, M., Brousseau, P., Auffret, M., Budzinski, H., Fournier, M., 2015. Genotoxic and immunotoxic potential effects of selected psychotropic drugs and antibiotics on blue mussel (Mytilus edulis) hemocytes. Environ. Pollut. 202, 177–186. https://doi.org/10.1016/j.envpol.2015.03.025

Lacoste, A., Malham, S.K., Cueff, A., Poulet, S.A., 2001. Noradrenaline reduces the stimulatory effect of interleukin-1α on reactive oxygen species production by oyster immunocytes. Invertebr. Biol. 120, 358–364. https://doi.org/10.1111/j.1744-7410.2001.tb00043.x

Li, H.-D., Xu, Q.-S., Liang, Y.-Z., 2018. libPLS: An integrated library for partial least squares regression and linear discriminant analysis. Chemom. Intell. Lab. Syst. 176, 34–43. https://doi.org/10.1016/j.chemolab.2018.03.003

Liu, A., Wang, C., Hehir, M., Zhou, T., Yang, J., 2015. In vivo induction of CYP in mice by carbamazepine is independent on PXR. Pharmacol. Rep. 67, 299–304. https://doi.org/10.1016/j.pharep.2014.10.002

Liu, H., Sadygov, R.G., Yates, J.R., 2004. A model for random sampling and estimation of relative protein abundance in shotgun proteomics. Anal. Chem. 76, 4193–4201. https://doi.org/10.1021/ac0498563

Margot, J., Rossi, L., Barry, D.A., Holliger, C., 2015. A review of the fate of micropollutants in wastewater treatment plants. WIREs Water 2, 457–487. https://doi.org/10.1002/wat2.1090

Martin-Diaz, L., Franzellitti, S., Buratti, S., Valbonesi, P., Capuzzo, A., Fabbri, E., 2009. Effects of environmental concentrations of the antiepilectic drug carbamazepine on biomarkers and cAMP-mediated cell signaling in the mussel Mytilus galloprovincialis. Aquat. Toxicol. Amst. Neth. 94, 177–185. https://doi.org/10.1016/j.aquatox.2009.06.015

Martínez Bueno, M.J., Boillot, C., Fenet, H., Chiron, S., Casellas, C., Gómez, E., 2013. Fast and easy extraction combined with high resolution-mass spectrometry for residue analysis of two anticonvulsants and their transformation products in marine mussels. J. Chromatogr. A 1305, 27–34. https://doi.org/10.1016/j.chroma.2013.06.071

Martínez Bueno, M.J., Boillot, C., Munaron, D., Fenet, H., Casellas, C., Gómez, E., 2014. Occurrence of venlafaxine residues and its metabolites in marine mussels at trace levels: development of analytical method and a monitoring program. Anal. Bioanal. Chem. 406, 601–610. https://doi.org/10.1007/s00216-013-7477-x

Martínez Bueno, M.J., Herrera, S., Munaron, D., Boillot, C., Fenet, H., Chiron, S., Gómez, E., 2016. POCIS passive samplers as a monitoring tool for pharmaceutical residues and their transformation products in marine environment. Environ. Sci. Pollut. Res. 23, 5019–5029. https://doi.org/10.1007/s11356-014-3796-5

Martins, C., Dreij, K., Costa, P.M., 2019. The State-of-the Art of Environmental Toxicogenomics: Challenges and Perspectives of “Omics” Approaches Directed to Toxicant Mixtures. Int. J. Environ. Res. Public. Health 16, 4718. https://doi.org/10.3390/ijerph16234718

Mezzelani, M., Gorbi, S., Regoli, F., 2018. Pharmaceuticals in the aquatic environments: Evidence of emerged threat and future challenges for marine organisms. Mar. Environ. Res. 140, 41–60. https://doi.org/10.1016/j.marenvres.2018.05.001

Moreno-González, R., Rodríguez-Mozaz, S., Huerta, B., Barceló, D., León, V.M., 2016. Do pharmaceuticals bioaccumulate in marine molluscs and fish from a coastal lagoon? Environ. Res. 146, 282–298. https://doi.org/10.1016/j.envres.2016.01.001

Perez-Riverol, Y., Csordas, A., Bai, J., Bernal-Llinares, M., Hewapathirana, S., Kundu, D.J., Inuganti, A., Griss, J., Mayer, G., Eisenacher, M., Pérez, E., Uszkoreit, J., Pfeuffer, J., Sachsenberg, T., Yılmaz, Ş., Tiwary, S., Cox, J., Audain, E., Walzer, M., Jarnuczak, A.F., Ternent, T., Brazma, A., Vizcaíno, J.A., 2019. The PRIDE database and related tools and resources in 2019: improving support for quantification data. Nucleic Acids Res. 47, D442–D450. https://doi.org/10.1093/nar/gky1106

Ramirez, G., Gomez, E., Dumas, T., Rosain, D., Mathieu, O., Fenet, H., Courant, F., 2022. Early Biological Modulations Resulting from 1-Week Venlafaxine Exposure of Marine Mussels Mytilus galloprovincialis Determined by a Metabolomic Approach. Metabolites 12, 197. https://doi.org/10.3390/metabo12030197

Regoli, F., Giuliani, M.E., 2014. Oxidative pathways of chemical toxicity and oxidative stress biomarkers in marine organisms. Mar. Environ. Res., Sensing the marine environment using different animal models and levels of complexity 93, 106–117. https://doi.org/10.1016/j.marenvres.2013.07.006

Santos, L.H.M.L.M., Araújo, A.N., Fachini, A., Pena, A., Delerue-Matos, C., Montenegro, M.C.B.S.M., 2010. Ecotoxicological aspects related to the presence of pharmaceuticals in the aquatic environment. J. Hazard. Mater. 175, 45–95. https://doi.org/10.1016/j.jhazmat.2009.10.100

Schmidt, W., O’Rourke, K., Hernan, R., Quinn, B., 2011. Effects of the pharmaceuticals gemfibrozil and diclofenac on the marine mussel (Mytilus spp.) and their comparison with standardized toxicity tests. Mar. Pollut. Bull. 62, 1389–1395. https://doi.org/10.1016/j.marpolbul.2011.04.043

Schwarz, D.S., Blower, M.D., 2016. The endoplasmic reticulum: structure, function and response to cellular signaling. Cell. Mol. Life Sci. 73, 79–94. https://doi.org/10.1007/s00018-015-2052-6

Simmons, D.B.D., Miller, J., Clarence, S., McCallum, E.S., Balshine, S., Chandramouli, B., Cosgrove, J., Sherry, J.P., 2017. Altered expression of metabolites and proteins in wild and caged fish exposed to wastewater effluents in situ. Sci. Rep. 7, 17000. https://doi.org/10.1038/s41598-017-12473-6

Smith, C.A., Want, E.J., O’Maille, G., Abagyan, R., Siuzdak, G., 2006. XCMS: Processing Mass Spectrometry Data for Metabolite Profiling Using Nonlinear Peak Alignment, Matching, and Identification. Anal. Chem. 78, 779–787. https://doi.org/10.1021/ac051437y

Song, Q., Chen, H., Li, Y., Zhou, H., Han, Q., Diao, X., 2016. Toxicological effects of benzo(a)pyrene, DDT and their mixture on the green mussel Perna viridis revealed by proteomic and metabolomic approaches. Chemosphere 144, 214–224. https://doi.org/10.1016/j.chemosphere.2015.08.029

Sousa, J.C.G., Barbosa, M.O., Ribeiro, A.R.L., Ratola, N., Pereira, M.F.R., Silva, A.M.T., 2020. Distribution of micropollutants in estuarine and sea water along the Portuguese coast. Mar. Pollut. Bull. 154, 111120. https://doi.org/10.1016/j.marpolbul.2020.111120

Szklarczyk, D., Gable, A.L., Lyon, D., Junge, A., Wyder, S., Huerta-Cepas, J., Simonovic, M., Doncheva, N.T., Morris, J.H., Bork, P., Jensen, L.J., Mering, C. von, 2019. STRING v11: protein-protein association networks with increased coverage, supporting functional discovery in genome-wide experimental datasets. Nucleic Acids Res. 47, D607–D613. https://doi.org/10.1093/nar/gky1131

Trapp, J., Armengaud, J., Pible, O., Gaillard, J.-C., Abbaci, K., Habtoul, Y., Chaumot, A., Geffard, O., 2015. Proteomic Investigation of Male Gammarus fossarum, a Freshwater Crustacean, in Response to Endocrine Disruptors. J. Proteome Res. 14, 292–303. https://doi.org/10.1021/pr500984z

Trapp, J., Gouveia, D., Almunia, C., Pible, O., Degli Esposti, D., Gaillard, J.-C., Chaumot, A., Geffard, O., Armengaud, J., 2018. Digging Deeper Into the Pyriproxyfen-Response of the Amphipod Gammarus fossarum With a Next-Generation Ultra-High-Field Orbitrap Analyser: New Perspectives for Environmental Toxicoproteomics. Front. Environ. Sci. 6. https://doi.org/10.3389/fenvs.2018.00054

Vandenbrouck, T., Soetaert, A., van der Ven, K., Blust, R., De Coen, W., 2009. Nickel and binary metal mixture responses in Daphnia magna: Molecular fingerprints and (sub)organismal effects. Aquat. Toxicol. 92, 18–29. https://doi.org/10.1016/j.aquatox.2008.12.012

Vernouillet, G., Eullaffroy, P., Lajeunesse, A., Blaise, C., Gagné, F., Juneau, P., 2010. Toxic effects and bioaccumulation of carbamazepine evaluated by biomarkers measured in organisms of different trophic levels. Chemosphere 80, 1062–1068. https://doi.org/10.1016/j.chemosphere.2010.05.010

Want, E.J., Wilson, I.D., Gika, H., Theodoridis, G., Plumb, R.S., Shockcor, J., Holmes, E., Nicholson, J.K., 2010. Global metabolic profiling procedures for urine using UPLC–MS. Nat. Protoc. 5, 1005–1018. https://doi.org/10.1038/nprot.2010.50

Weissbach, H., Etienne, F., Hoshi, T., Heinemann, S.H., Lowther, W.T., Matthews, B., St. John, G., Nathan, C., Brot, N., 2002. Peptide Methionine Sulfoxide Reductase: Structure, Mechanism of Action, and Biological Function. Arch. Biochem. Biophys. 397, 172–178. https://doi.org/10.1006/abbi.2001.2664

Wishart, D.S., Jewison, T., Guo, A.C., Wilson, M., Knox, C., Liu, Y., Djoumbou, Y., Mandal, R., Aziat, F., Dong, E., Bouatra, S., Sinelnikov, I., Arndt, D., Xia, J., Liu, P., Yallou, F., Bjorndahl, T., Perez-Pineiro, R., Eisner, R., Allen, F., Neveu, V., Greiner, R., Scalbert, A., 2013. HMDB 3.0—The Human Metabolome Database in 2013. Nucleic Acids Res. 41, D801–D807. https://doi.org/10.1093/nar/gks1065

Wright, J.C., Choudhary, J.S., 2016. DecoyPyrat: Fast Non-redundant Hybrid Decoy Sequence Generation for Large Scale Proteomics. J. Proteomics Bioinform. 9, 176–180. https://doi.org/10.4172/jpb.1000404

Xia, J., Wishart, D.S., 2010. MetPA: a web-based metabolomics tool for pathway analysis and visualization. Bioinforma. Oxf. Engl. 26, 2342–2344. https://doi.org/10.1093/bioinformatics/btq418

Ying, W., 2008. NAD+/NADH and NADP+/NADPH in cellular functions and cell death: regulation and biological consequences. Antioxid. Redox Signal. 10, 179–206. https://doi.org/10.1089/ars.2007.1672